

Ay 127
Galaxy Clusters

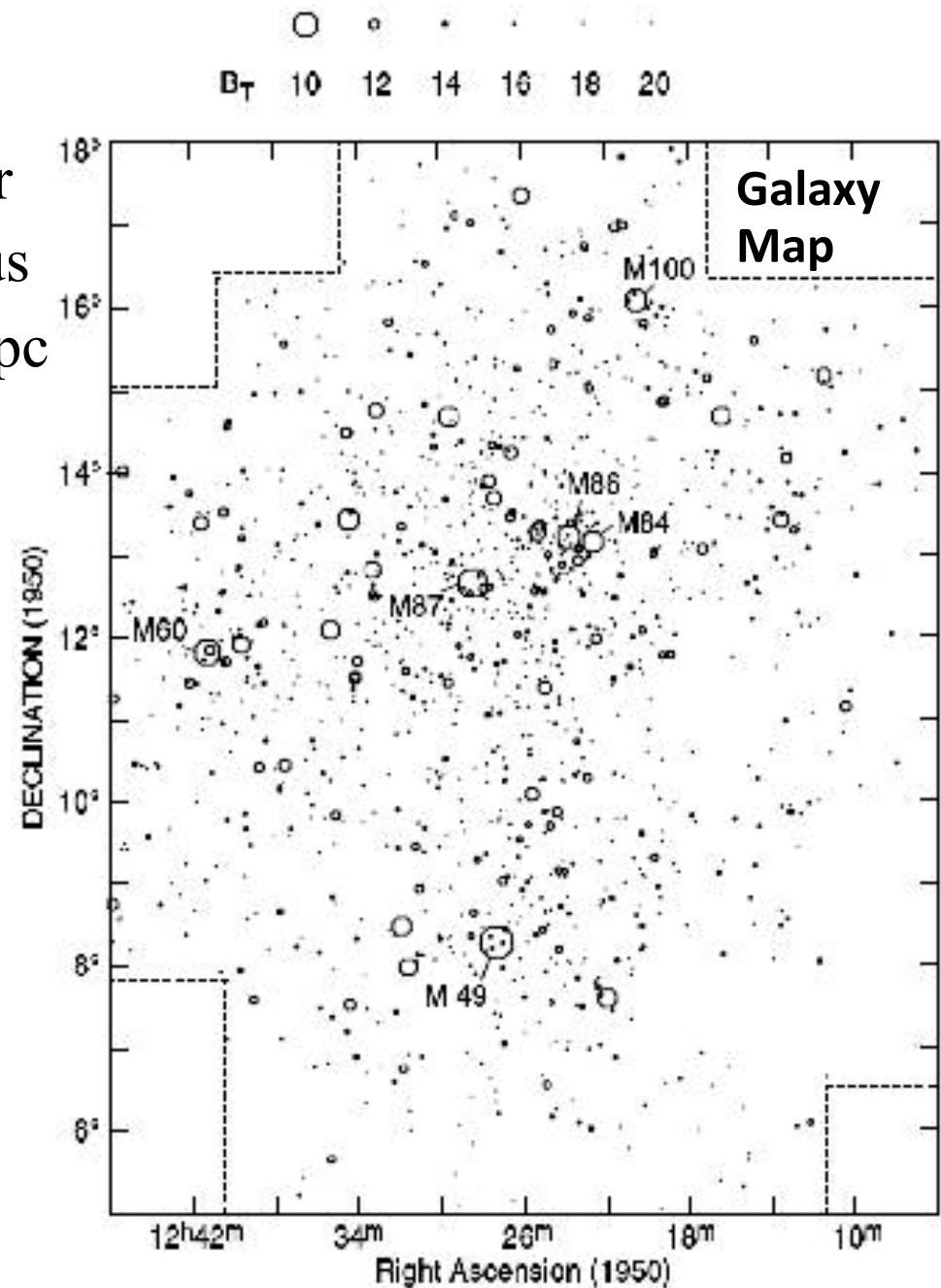
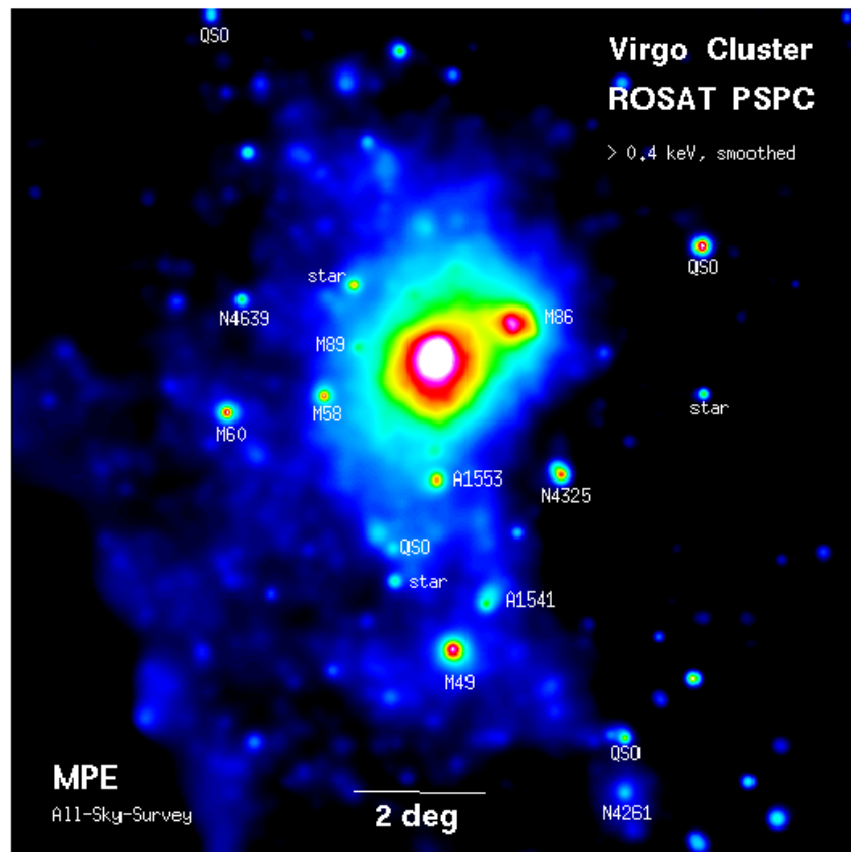


Clusters of Galaxies:

- Clusters are perhaps the most striking elements of the LSS
- Typically a few Mpc across, contain $\sim 100 - 1000$ luminous galaxies and many more dwarfs, masses $\sim 10^{14} - 10^{15} M_{\odot}$
- Gravitationally bound, but may not be fully virialized
- Filled with hot X-ray gas, mass of the gas may exceed the mass of stars in cluster galaxies
- Dark matter is the dominant mass component ($\sim 80 - 85\%$)
- Only $\sim 10 - 20\%$ of galaxies live in clusters, but it is hard to draw the line between groups and clusters, and at least $\sim 50\%$ of all galaxies are in clusters or groups
- Clusters have higher densities than groups, contain a majority of E's and S0's while groups are dominated by spirals
- Interesting galaxy evolution processes happen in clusters

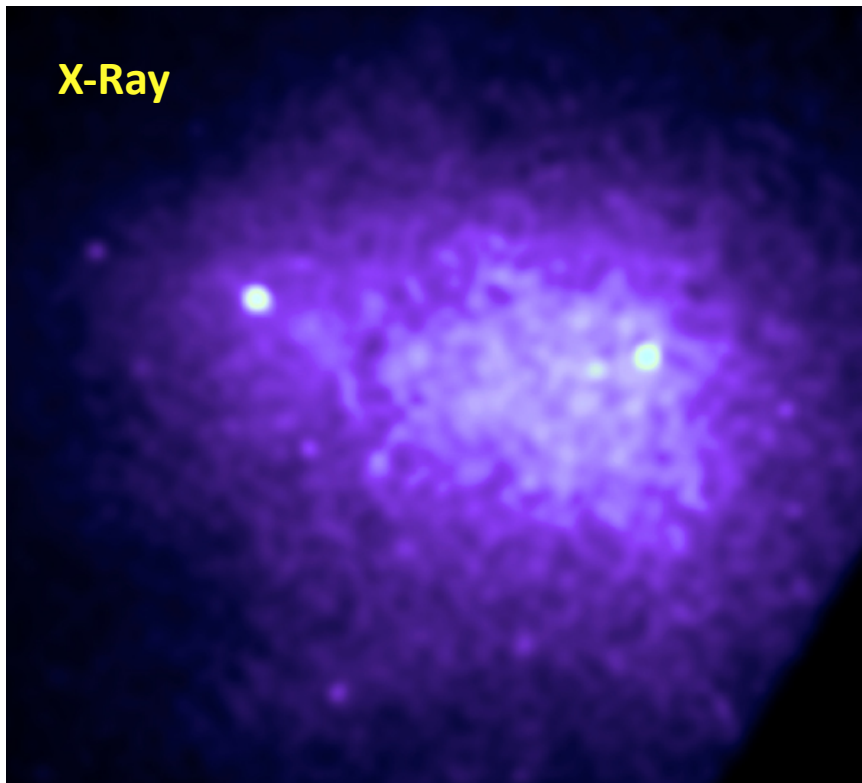
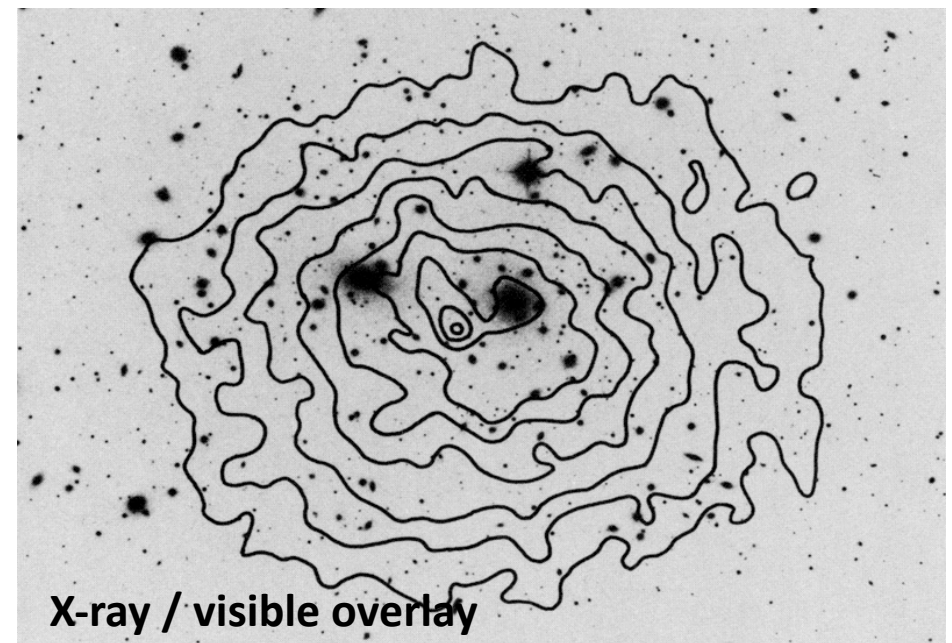
The Virgo Cluster:

- Irregular, relatively poor cluster
- Distance ~ 16 Mpc, closest to us
- Diameter $\sim 10^\circ$ on the sky, 3 Mpc
- ~ 2000 galaxies, mostly dwarfs

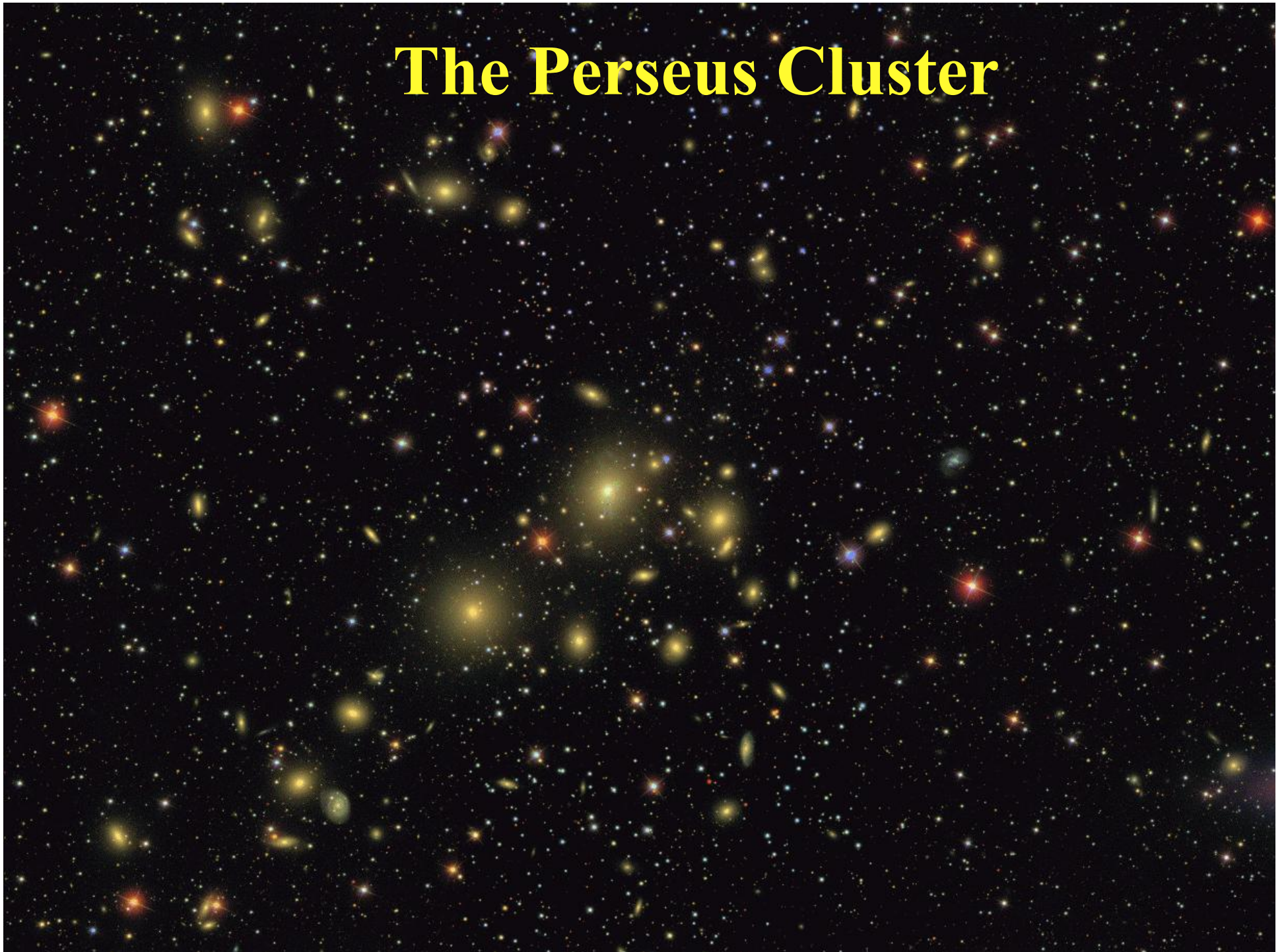


The Coma Cluster

- Nearest rich cluster, with $>10,000$ galaxies
- Distance ~ 90 Mpc
- Diameter $\sim 4\text{-}5^\circ$ on the sky, 6-8 Mpc



The Perseus Cluster

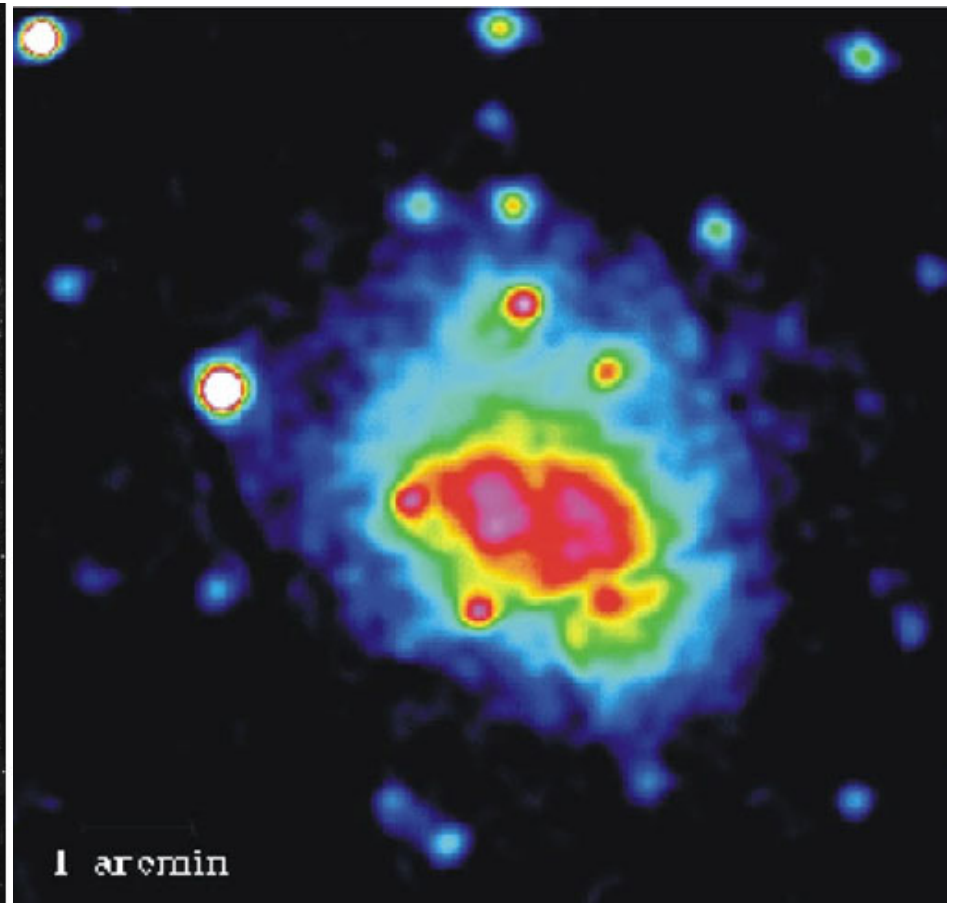


A Very Distant Cluster 0939+4713 ($z = 0.41$)

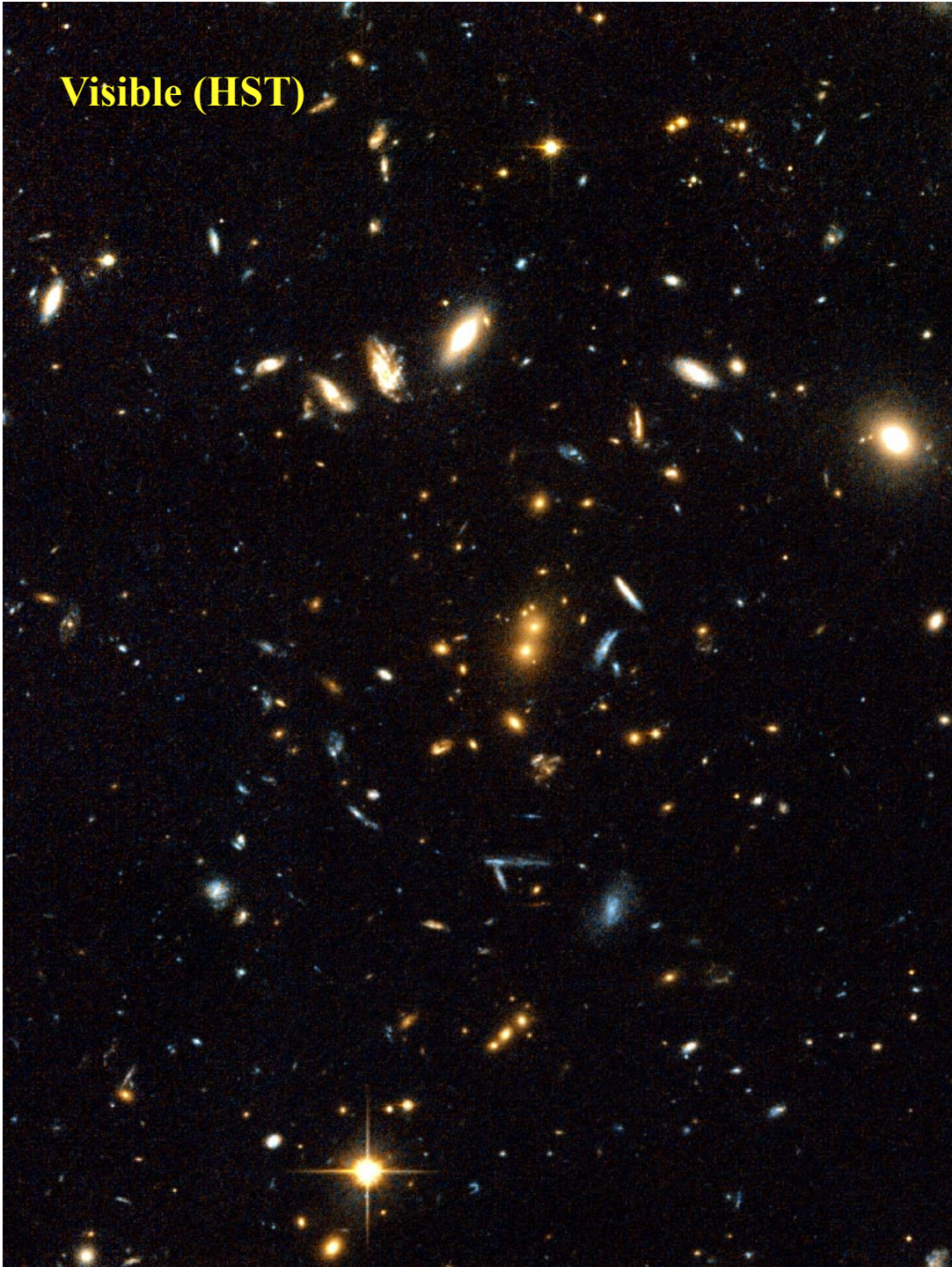
Visible (HST)



X-Ray (Rosat)

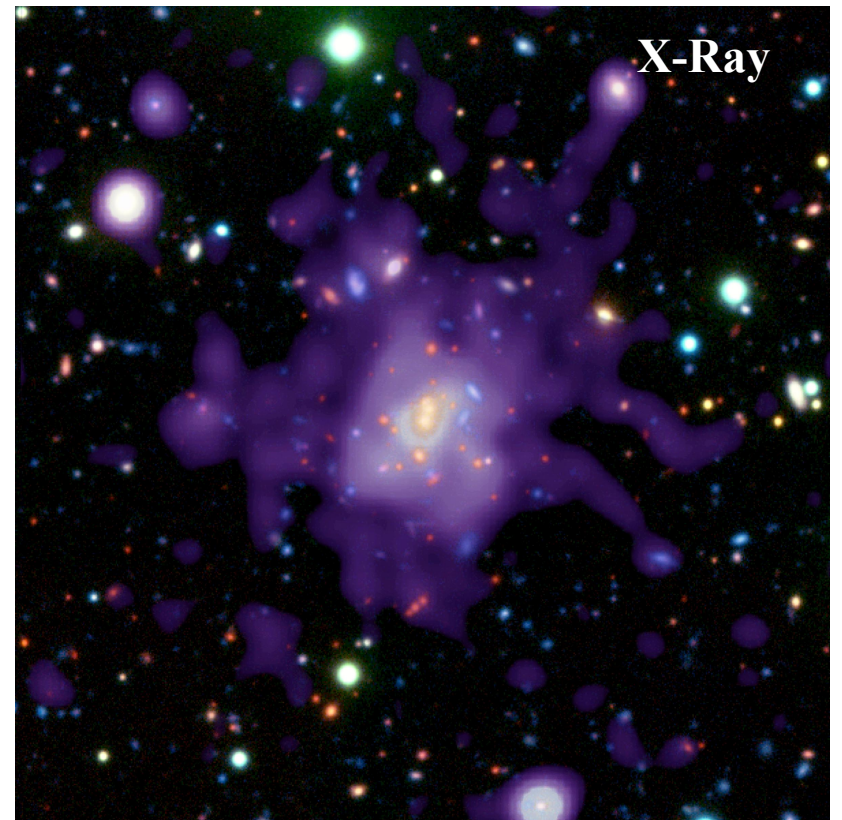


Visible (HST)



**One of the most
distant clusters now
known, 1252-2927
($z = 1.24$)**

X-Ray



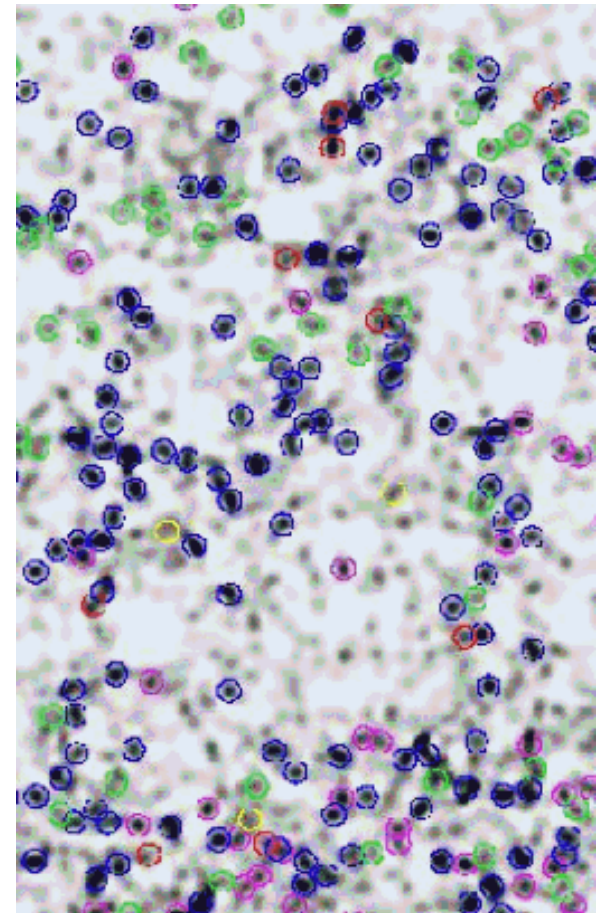
Surveys for Galaxy Clusters

Galaxy clusters contain galaxies, hot gas, and dark matter

Can survey for each of these components using observations in different wavebands:

1. Optical

- Look for an overdensity of galaxies in patches on the sky
- Can use color information (clusters contain many red elliptical galaxies)
- At higher redshifts, use redder bands (IR)
- **Disadvantages:** vulnerable to projection effects, rich cluster in the optical may not have especially high mass



Abell Cluster Catalog

- Nearby clusters cataloged by Abell (1958), extended to southern hemisphere by Abell et al. (1989)
 - By visual inspection of the POSS (& ESO) plates
 - Define region of radius $1.5h^{-1}$ (Abell radius)
 - Count galaxies within R_A between with an apparent magnitude between m_3 and $m_3 + 2$ (where m_3 is the magnitude of the 3rd brightest cluster member)
- Abell cataloged 4073 rich clusters (2712 in north)
- Richness class defined by number of galaxies with $m < m_3 + 2$ over background
 - Richness class 1-2-3-4 correspond to $N = 50-80-130-200$ galaxies
 - Most clusters are poor (richness class 0), catalog is incomplete here
- Extended by more modern work, e.g., $\sim 20,000$ clusters from DPOSS (Gal et al.)

Clusters From Photographic Digital Sky Surveys

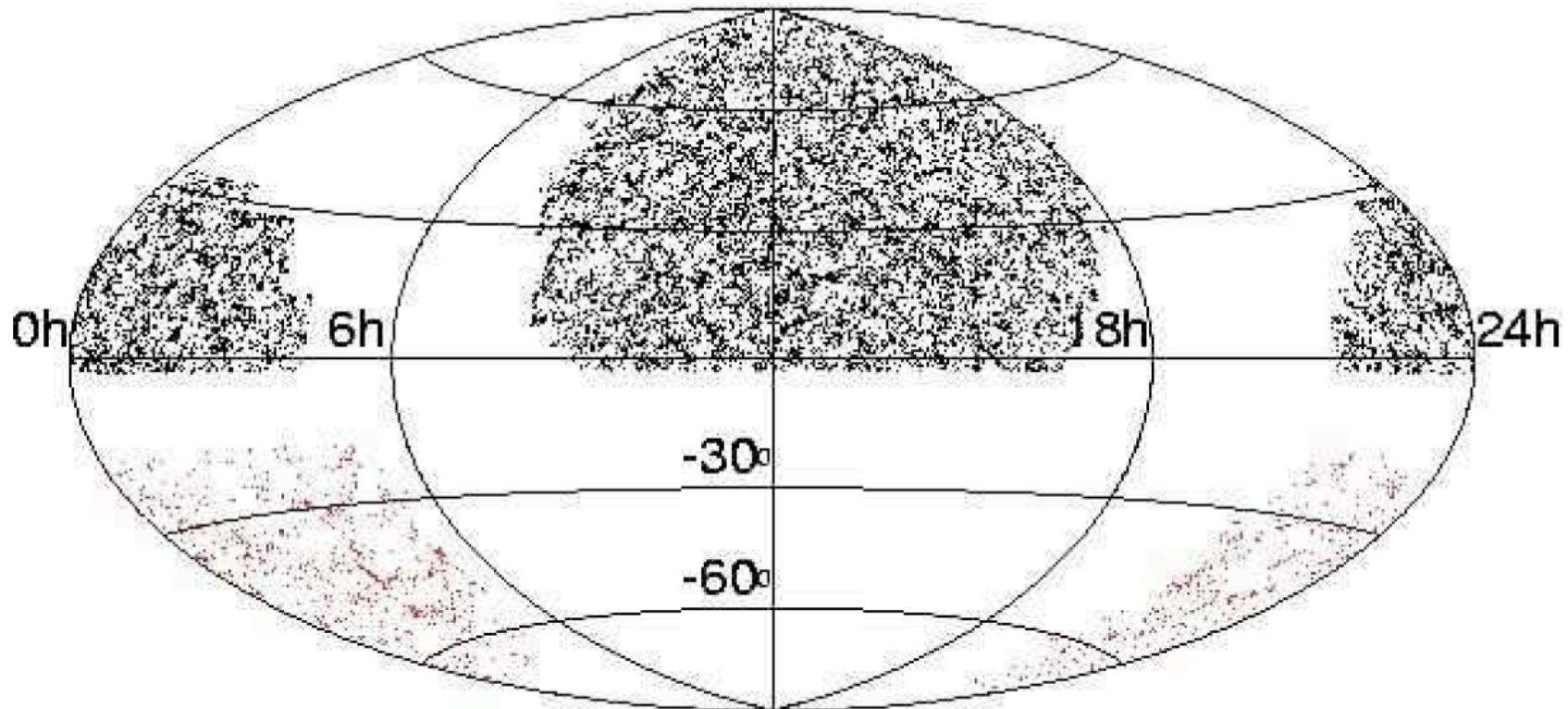
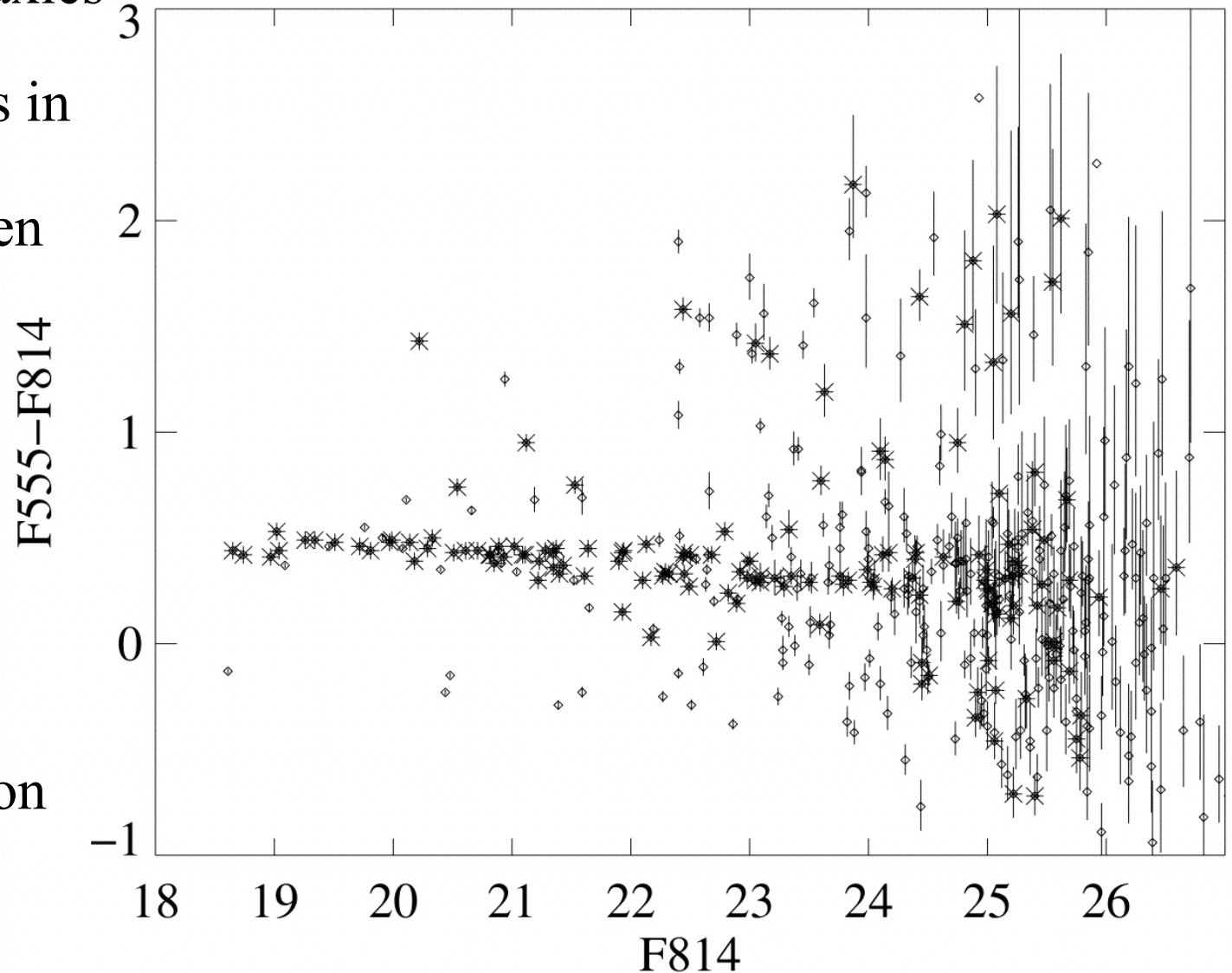


Fig. 2. The sky distribution of NoSOCS (northern sky) and APM (southern sky) candidate clusters in equatorial coordinates. The much higher density of NoSOCS is due to its deeper photometry and lower richness limit.

The Red Sequence Technique

- Exploit the color-magnitude (i.e., \sim mass-metallicity) relation for early-type galaxies
- Select galaxies in the right color band for a given redshift
- The sequence changes in redshift due to the K-correction



The “Cut and Enhance” Technique

Use the color cut to select likely early-type galaxies, then smooth

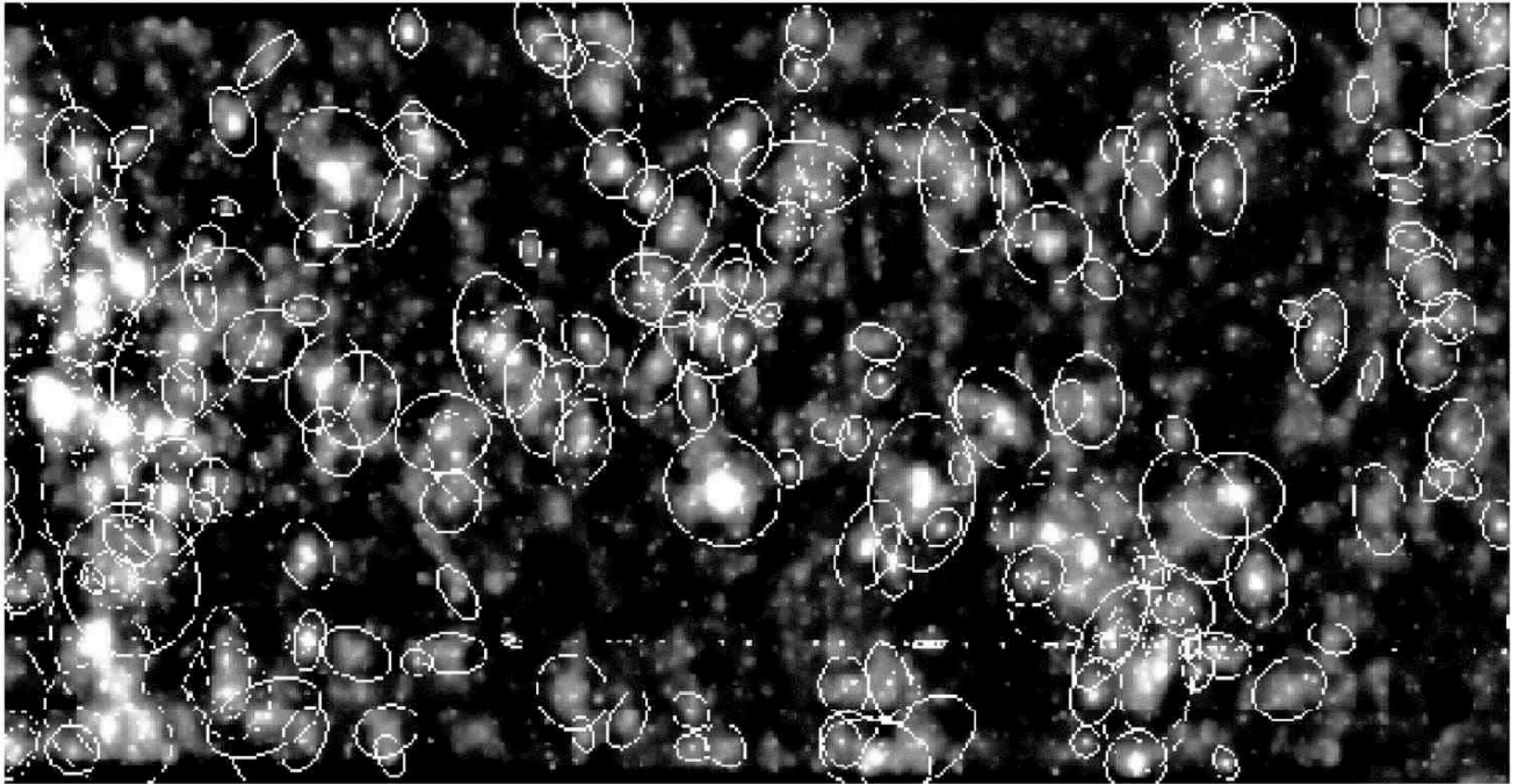
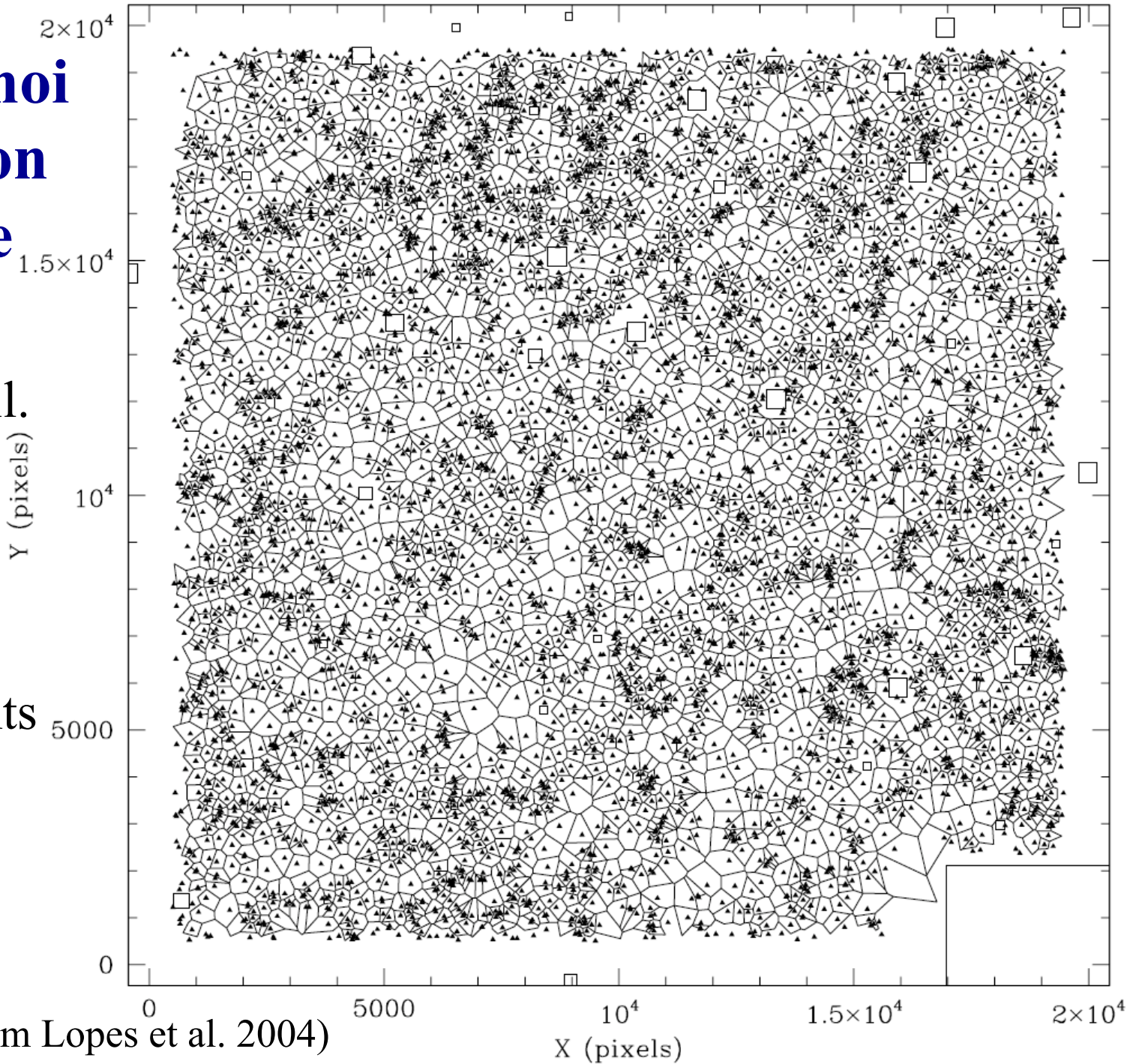


Fig. 4. An enhanced map of the galaxy distribution in the SDSS Early Data Release, after applying the $g^* - r^* - i^*$ color-color cut. Detected clusters are circled. Taken from Goto *et al.* (2002).

The Voronoi Tessellation Technique

Each galaxy defines a cell.
Cell area
 $\sim 1/\text{density}$;
look for
density
enhancements



(DPOSS data, from Lopes et al. 2004)

Cluster Classifications

- Abell classified clusters as:
 - Regular: \sim circularly symmetrical w/ a central concentration, members are predominantly E/S0's (e.g., Coma)
 - Irregular: \sim less well defined structure, more spirals (e.g., Hercules, Virgo)
- Bautz-Morgan classification scheme (1970), based on brightest galaxy in cluster:
 - I: Cluster has centrally located cD galaxy
 - II: central galaxy is somewhere between a cD and a giant elliptical galaxy (e.g., Coma)
 - III: cluster has no dominant central galaxy
- Oemler (1974) classified clusters by galaxy content:
 - cD clusters: 1 or two dominant cD galaxies, E:S0:S \sim 3:4:2
 - Spiral rich: E:SO:S \sim 1:2:3 (similar to the field)
 - Spiral poor: no dominant cD, E:S0:S \sim 1:2:1

Some important trends:

- Spatial distribution of galaxies:
 - cD and regular clusters: spatial distribution is smooth and circularly symmetric, space density increases rapidly towards cluster center
 - Spiral-rich and irregular clusters are not symmetric, little central concentration. Spatial density is \sim uniform
- Morphological segregation:
 - In spiral-rich clusters, radial distribution of E, SO, Sp galaxies is about the same
 - In cD and spiral-poor clusters, relative space density of spirals decreases rapidly to cluster core (morphology-density relation)

What does it all mean?

- Regular, cD clusters have had time to “relax” and reach dynamic equilibrium
- Intermediate and Irregular clusters are still in the process of coming together, have not yet reached dynamic equilibrium
- cD galaxies probably formed by merging in the central regions
 - Many show multiple nuclei, and have extended outer envelopes compared to luminous ellipticals, accrete additional material due to tidal stripping of other galaxies

Surveys for Galaxy Clusters

2. X-Ray

- Galaxy clusters contain hot gas, which radiates X-ray radiation due to bremsstrahlung
- Advantage: bremsstrahlung scales with density and temperature as $n^2 T^{1/2}$ - i.e. *quadratically* in the density. ***Much less*** vulnerable to accidental line-of-sight projection effects
- **Disadvantage:** still not detecting clusters based on mass

3. Sunyaev-Zeldovich effect

- Distortion of the CMB due to photons scattering off electrons in the cluster. Mass weighted measure, but really detects hot gas, not dark matter, and subject to messy hydrodynamics

4. Weak Gravitational Lensing

- Selection based on mass. Difficult observationally

Cluster Surveys in X-rays

30

M. ARNAUD

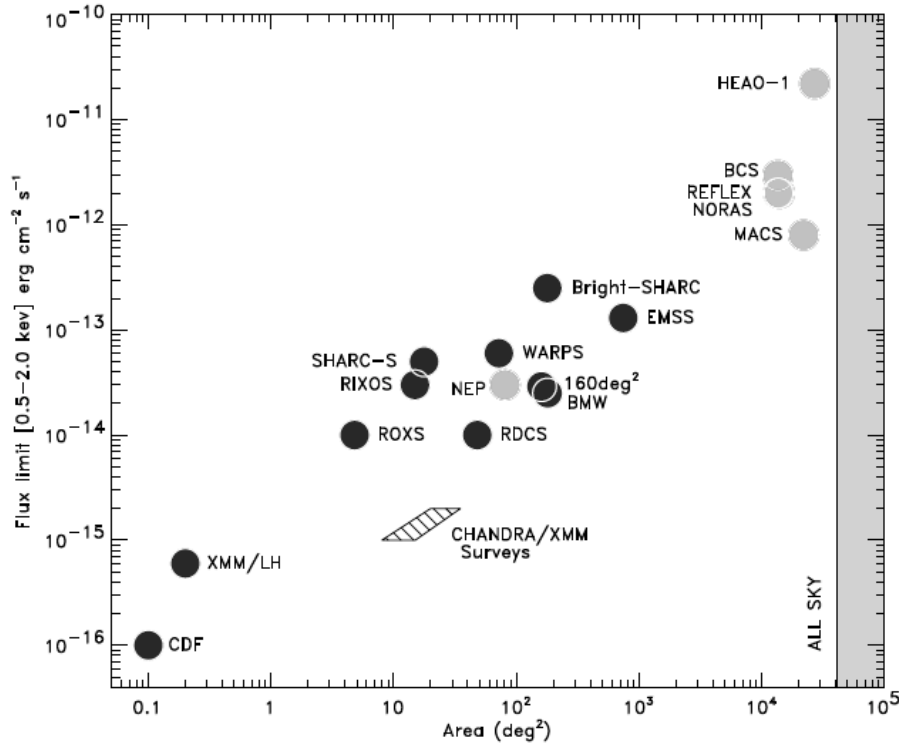


Fig. 28. – Solid angles and flux limits of various X-ray cluster surveys (references in text and in [150]). Dark filled circles: serendipitous surveys constructed from a collection of pointed observations. Light shaded circles: surveys covering contiguous areas. Figure from [150].

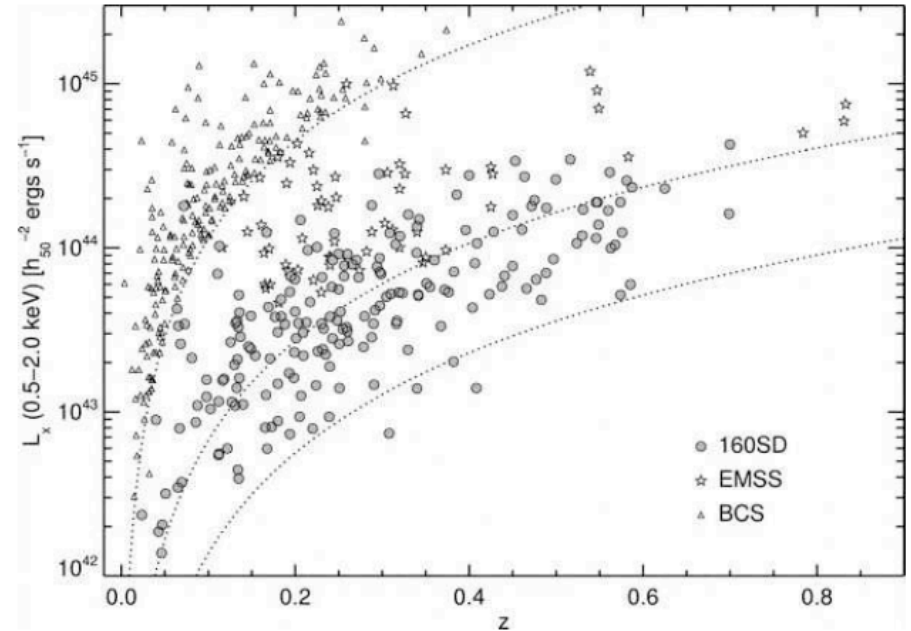


Fig. 29. – X-ray luminosity and redshift distribution of the 160SD [163], EMSS [159] and BCS [154] cluster samples. The dotted curves (left to right) are indicative flux limit of the surveys: $2.7 \cdot 10^{-12}$, $1.5 \cdot 10^{-13}$, $3 \cdot 10^{-14}$ ergs/cm²/s in the (0.5 – 2) keV energy band. Figure from [164]

Hot X-ray Gas in Clusters

- Virial equilibrium temperature $T \sim 10^7 - 10^8$ K, so emission is from free-free emission
- Many distant clusters are now being discovered via x-ray surveys
- Temperatures are not uniform, we see patches of “hot spots” which are not obviously associated with galaxies. May have been heated as smaller galaxies (or clumps of galaxies) fell into the cluster
- In densest regions, gas may cool and sink toward the cluster center as a “cooling flow”
- Unlikely that all of it has escaped from galaxies, some must be around from cluster formation process. It is heated via shocks as the gas falls into the cluster potential
- But some metals, metallicity $\sim 1/3$ Solar, must be from stars in galaxies
- X-ray luminosity correlates with cluster classification, regular clusters have high x-ray luminosity, irregular clusters have low x-ray luminosity

Virial Masses of Clusters:

Virial Theorem for a test particle (a galaxy, or a proton), moving in a cluster potential well:

$$E_k = E_p / 2 \quad \rightarrow \quad m_g \sigma^2 / 2 = G m_g M_{cl} / (2 R_{cl})$$

where σ is the velocity dispersion

Thus the cluster mass is: $M_{cl} = \sigma^2 R_{cl} / G$

Typical values for clusters: $\sigma \sim 500 - 1500 \text{ km/s}$

$$R_{cl} \sim 3 - 5 \text{ Mpc}$$

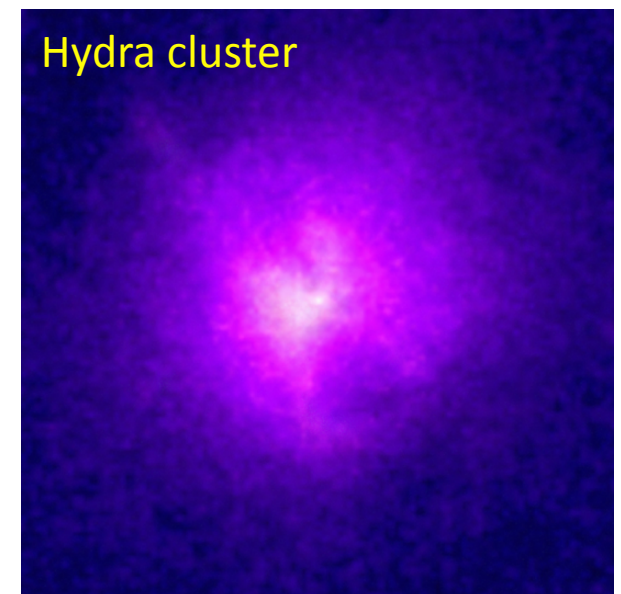
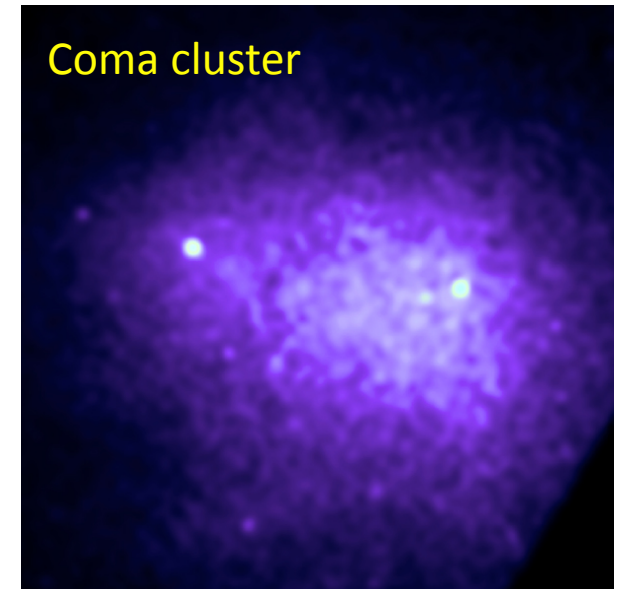
Thus, typical cluster masses are $M_{cl} \sim 10^{14} - 10^{15} M_{\odot}$

The typical cluster luminosities ($\sim 100 - 1000$ galaxies) are $L_{cl} \sim 10^{12} L_{\odot}$, and thus $(M/L) \sim 200 - 500$ in solar units

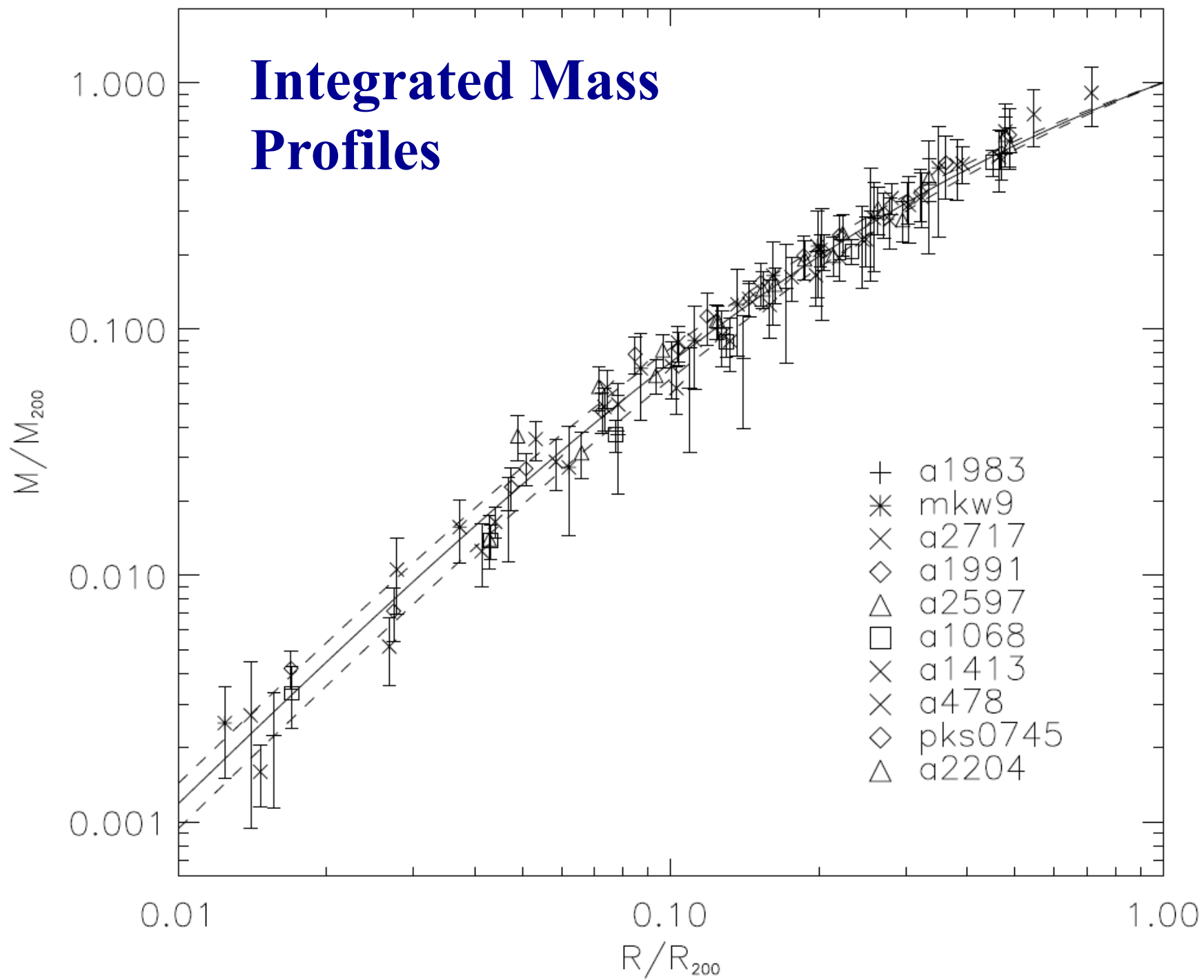
\rightarrow Lots of dark matter!

Masses of Clusters From X-ray Gas

- Note that for a proton moving in the cluster potential well with a $\sigma \sim 10^3$ km/s, $E_k = m_p \sigma^2 / 2 = 5 k T / 2 \sim$ few keV, and $T \sim$ few 10^7 °K \rightarrow **X-ray gas**
- Hydrostatic equilibrium requires:
$$M(r) = - kT / \mu m_H G (d \ln \rho / d \ln r) r$$
- If the cluster is \sim spherically symmetric this can be derived from X-ray intensity and spectral observations
- Typical cluster mass components from X-rays:
 - Total mass: 10^{14} to $10^{15} M_\odot$
 - Luminous mass: $\sim 5\%$
 - Gaseous mass: $\sim 10\%$
 - Dark matter: $\sim 85\%$

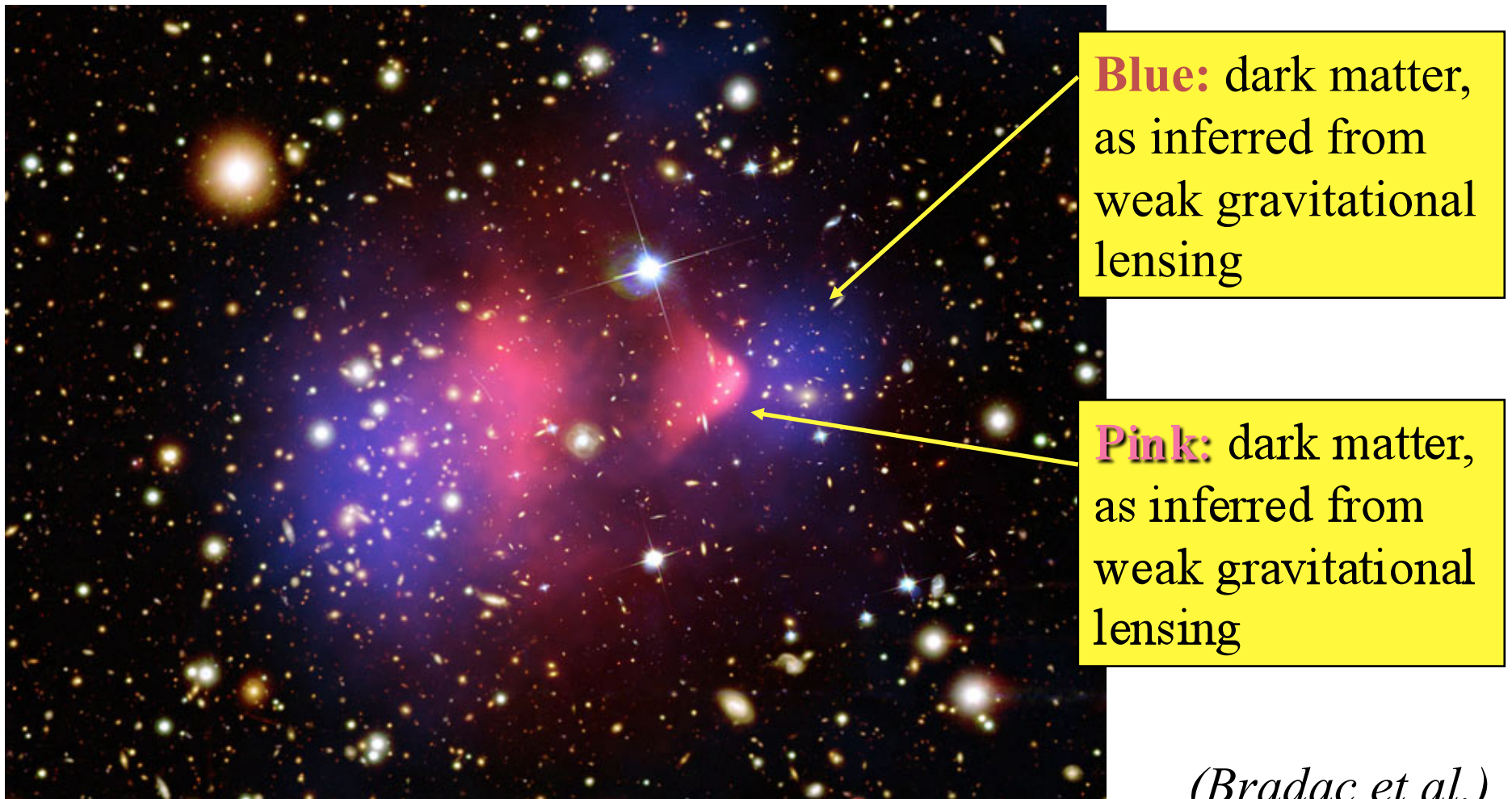


Integrated Mass Profiles



Dark Matter and X-Ray Gas in Cluster Mergers: The “Bullet Cluster” (1E 0657-56)

The dark matter clouds largely pass through each other, whereas the gas clouds collide and get shocked, and lag behind

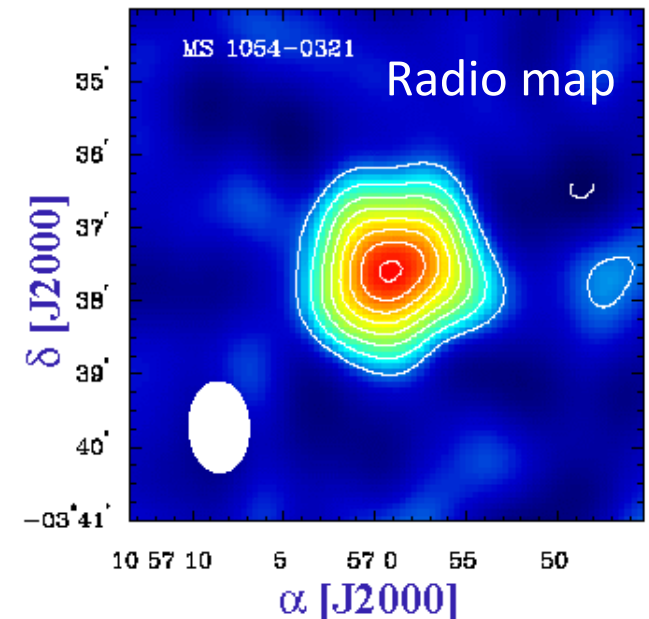
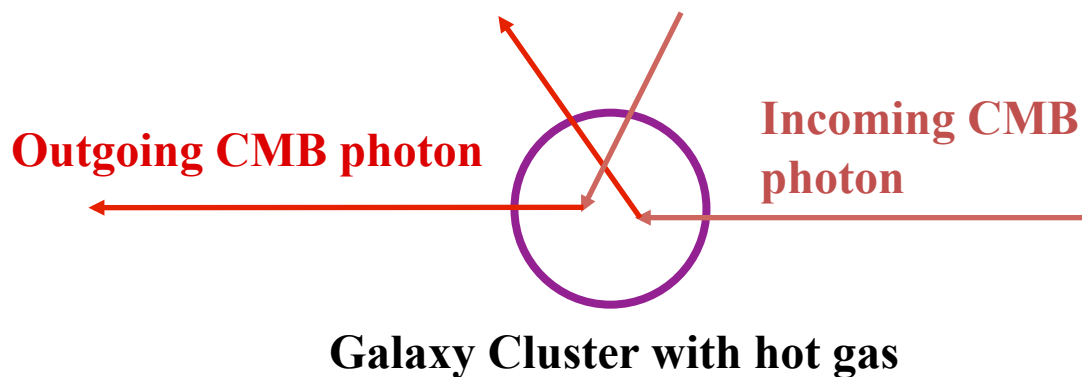
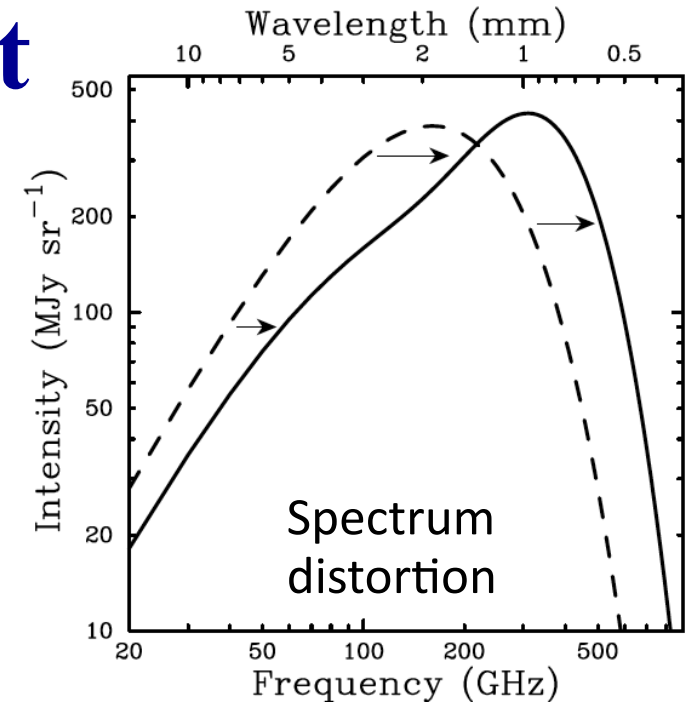




A 520

Synyaev-Zeldovich Effect

- Clusters of galaxies are filled with hot X-ray gas
- The electrons in the intracluster gas will scatter the background photons from the CMBR to higher energies and distort the blackbody spectrum
- This is detectable as a slight temperature dip or bump in the radio map of the cluster, against the uniform CMBR background



SZ Clusters from *Planck*

Keep an eye on the South Pole Telescope (SPT) as well

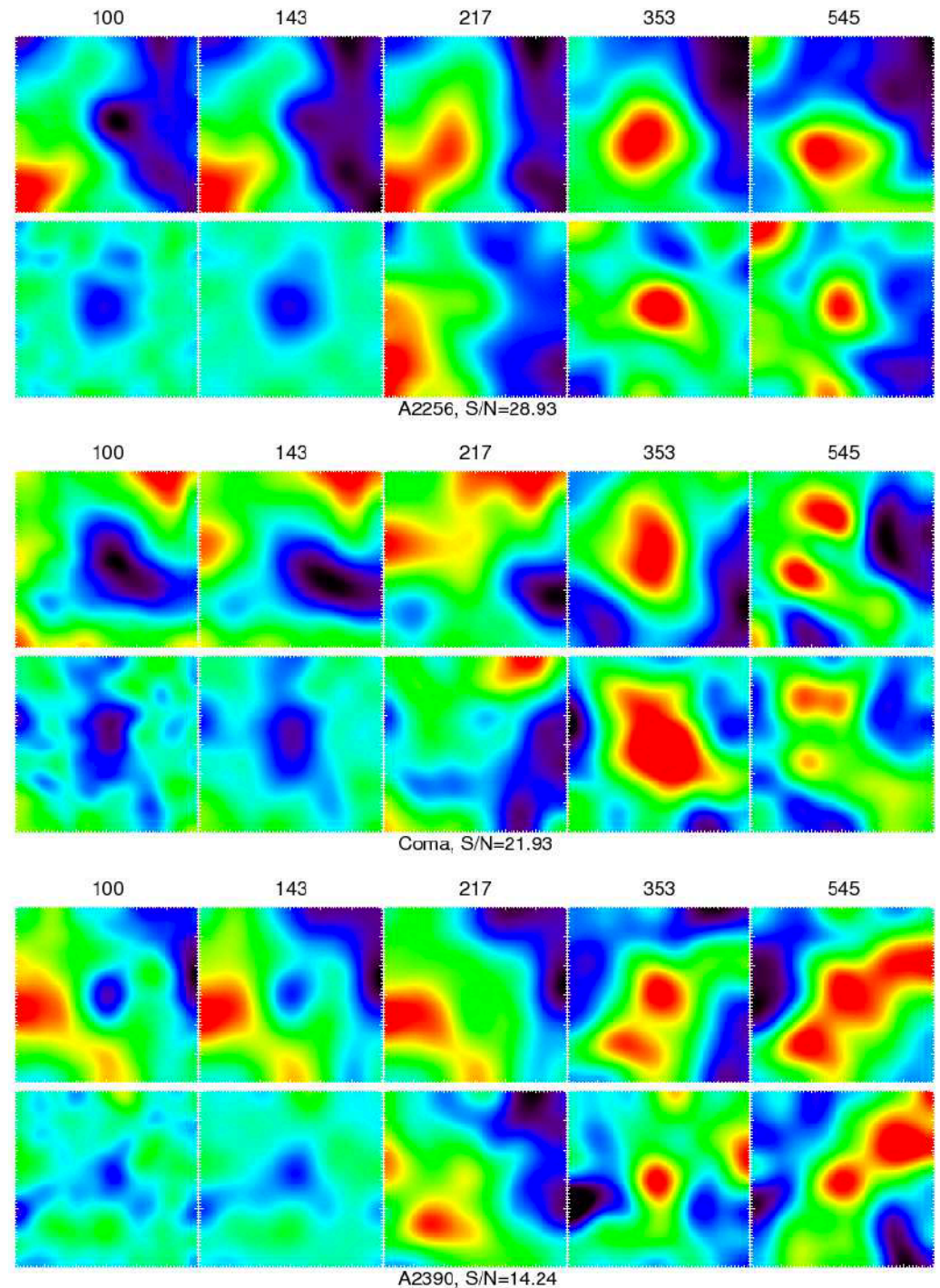
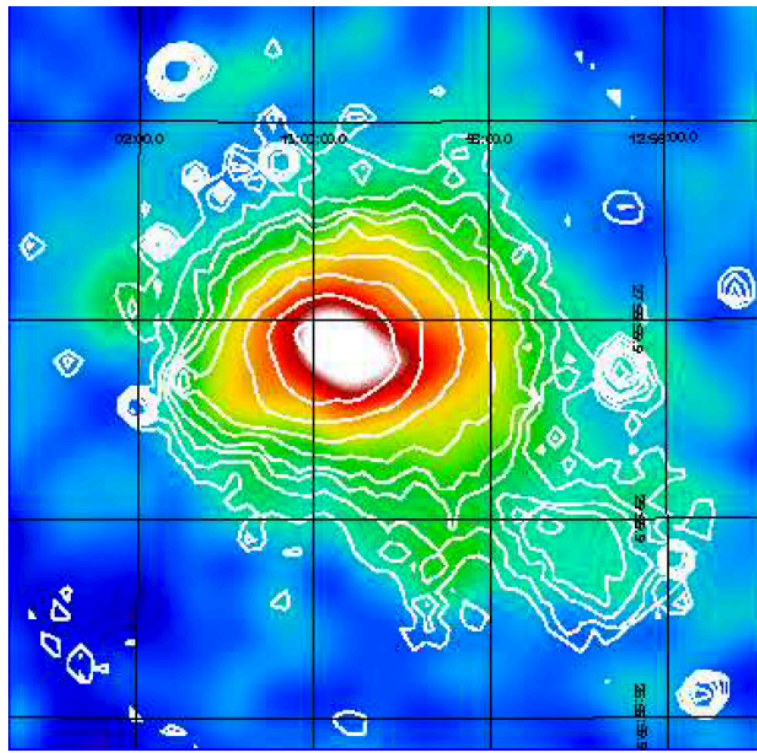


Fig. 1. *Planck* y-map of Coma on a $\sim 3^\circ \times 3^\circ$ patch with the *ROSAT-PSPC* iso-luminosity contours overlaid.

SZ Clusters from *Planck*

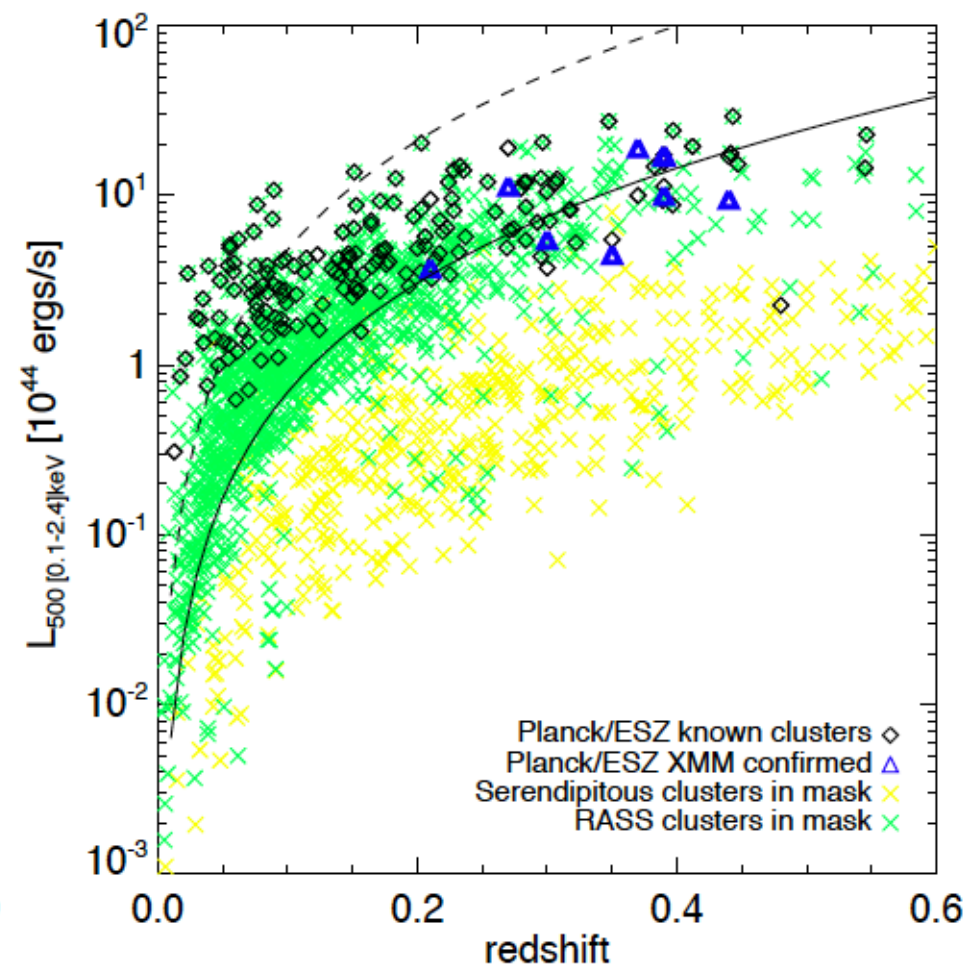
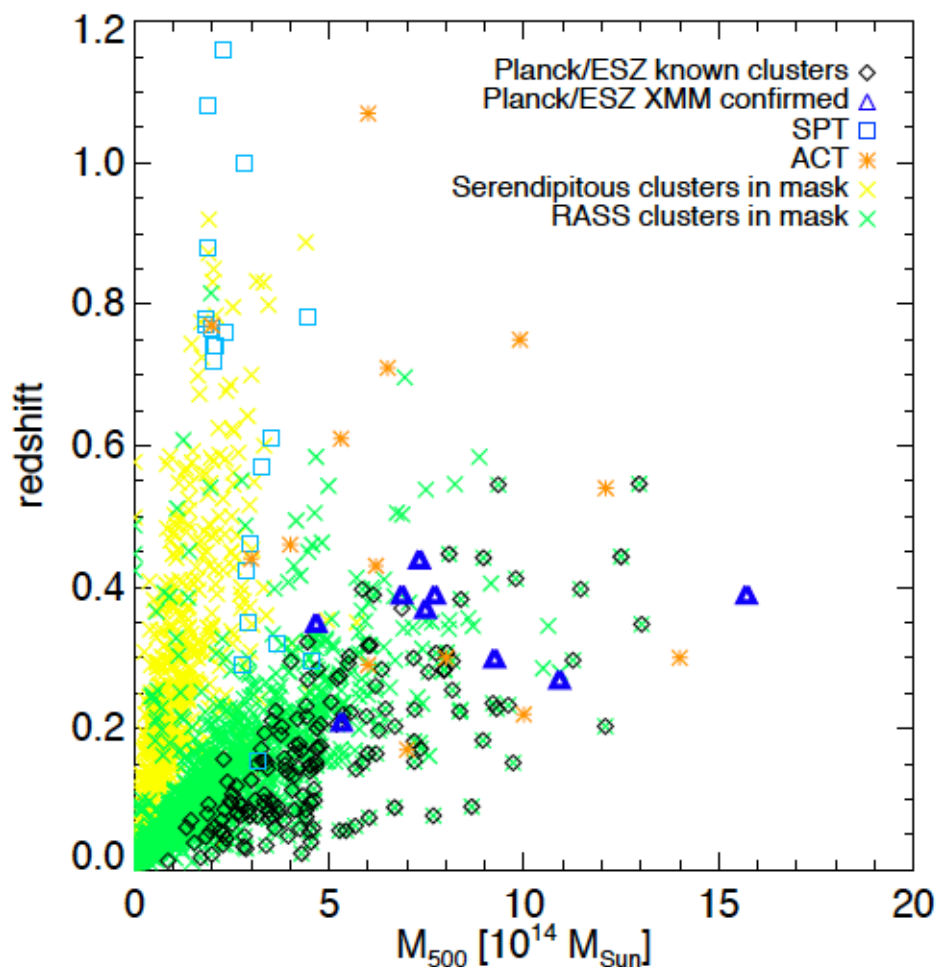
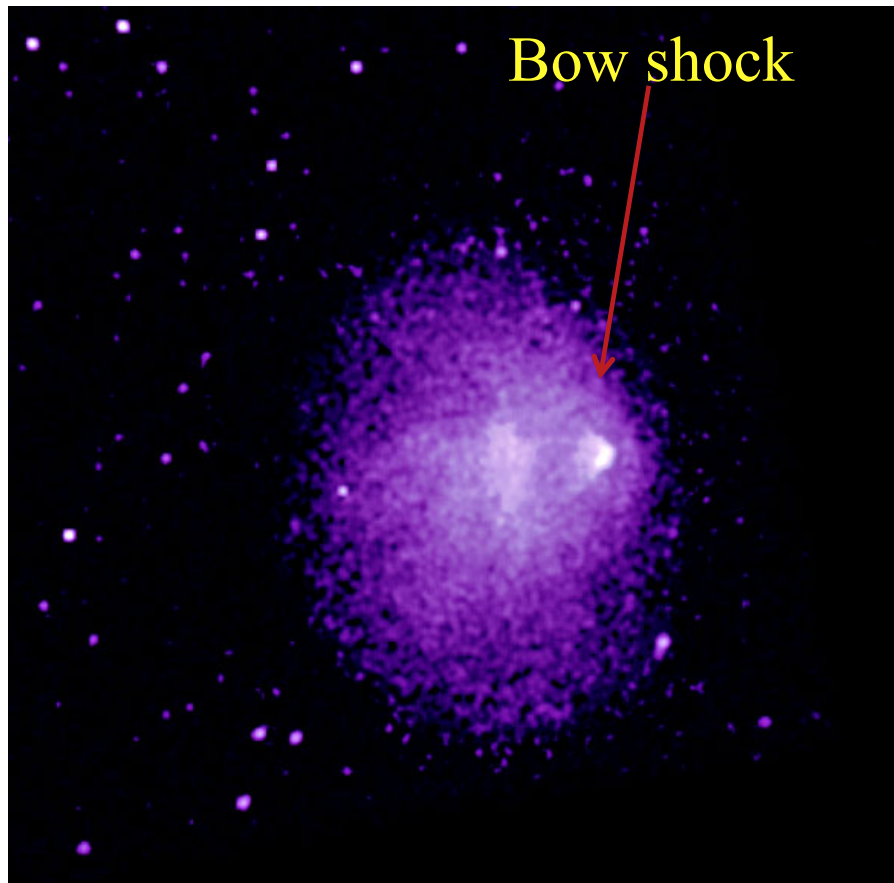


Fig. 20. The 158 clusters from the *Planck* ESZ sample identified with known X-ray clusters in redshift–mass space, compared with SPT and ACT samples from [Menanteau et al. \(2010\)](#); [Vanderlinde et al. \(2010\)](#), as well as serendipitous and RASS clusters

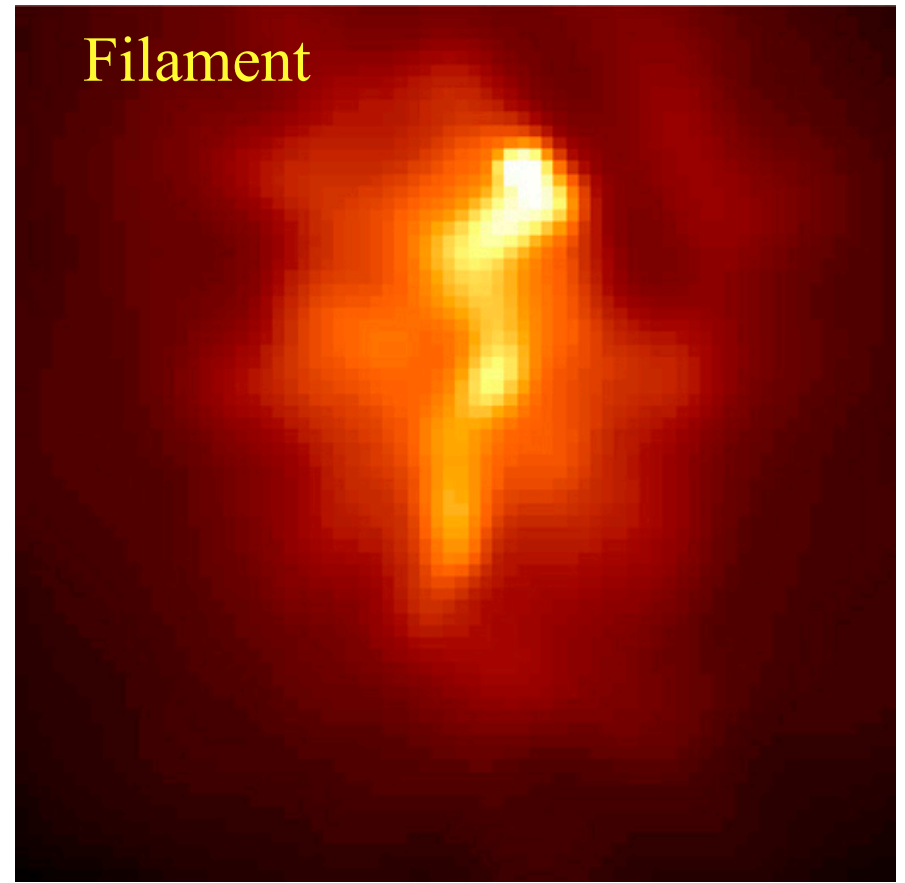
Fig. 21. The 158 clusters from the *Planck* ESZ sample identified with known X-ray clusters in redshift–luminosity space, compared with serendipitous and RASS clusters

Substructure in the X-Ray Gas

High resolution observations with *Chandra* show that many clusters have substructure in the X-ray surface brightness: hydrodynamical equilibrium is not a great approximation, clusters are still forming

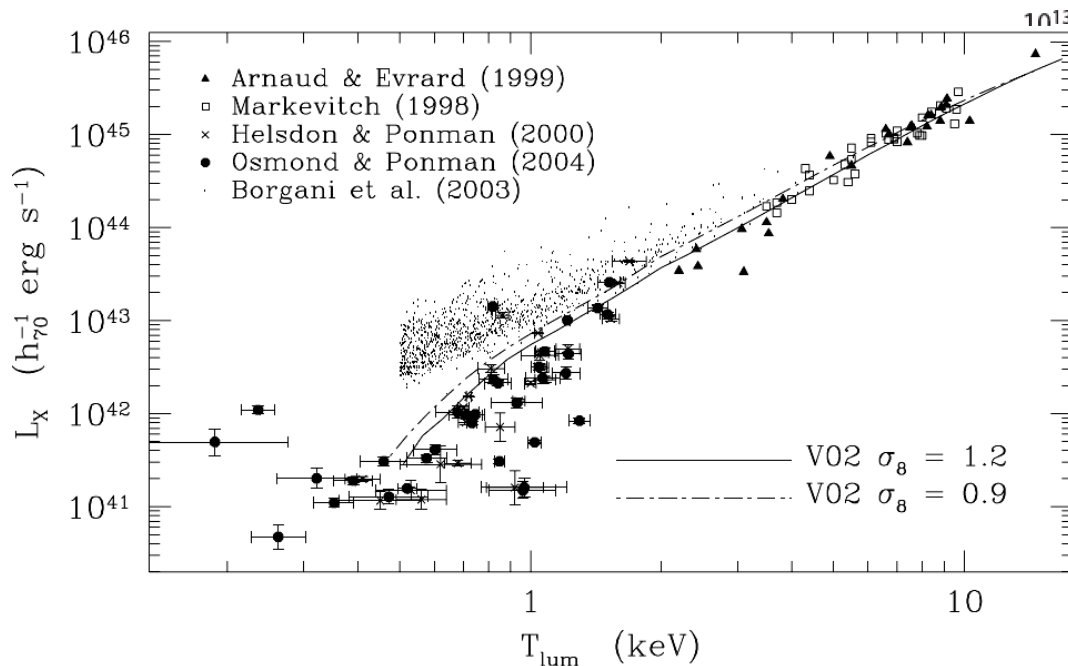


1E 0657-56

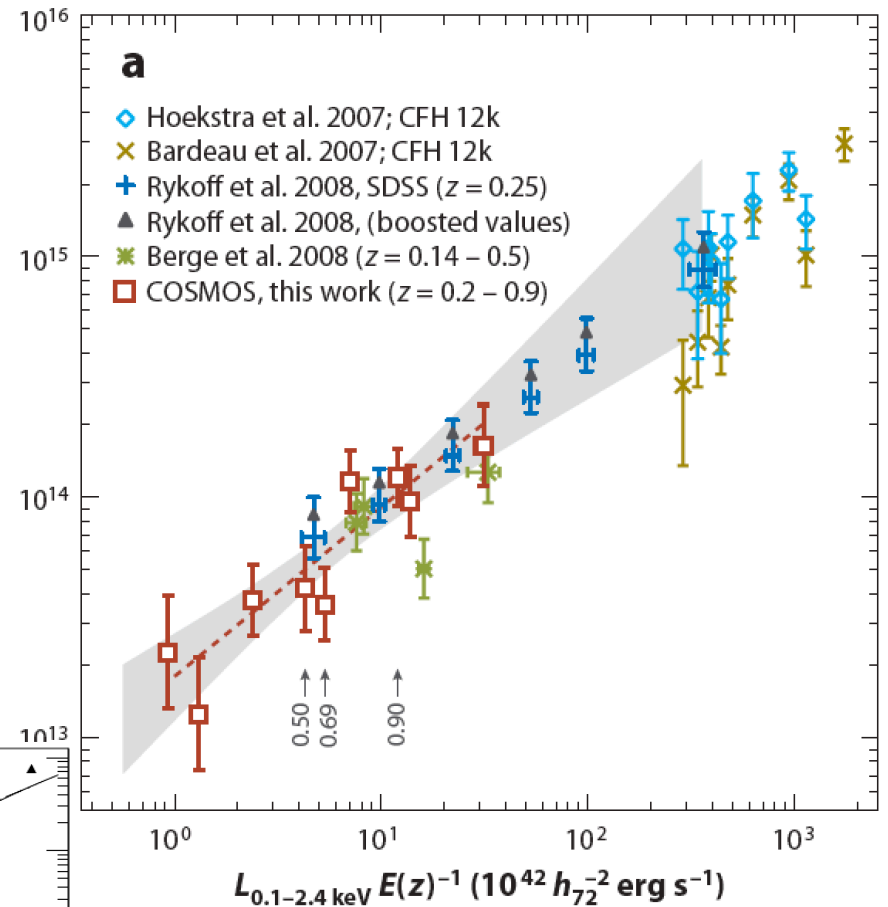


A 1795

Cluster X-Ray Luminosities Correlate With Mass



$M_{200} E(z) (h_{72}^{-1} M_{\odot})$



... and
Temperature

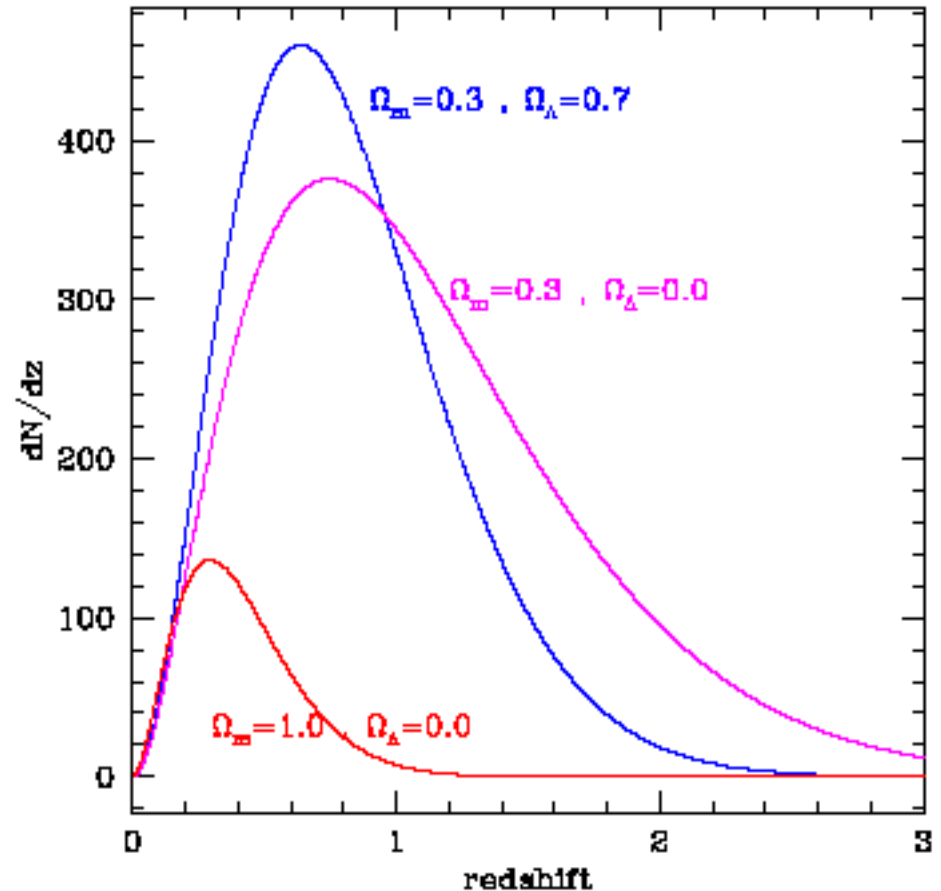
X-RAY OBSERVATIONS OF CLUSTERS OF GALAXIES

Relation	Slope	Expected in the standard self-similar model
L_X-T	2.64 ± 0.27	2
	2.88 ± 0.15	
$M_{\text{gas}}-T$	1.98 ± 0.18	1.5
	1.71 ± 0.13	
	1.89 ± 0.20	
	1.80 ± 0.16	
$EM-T$	1.38	0.5
$S-T$	0.65 ± 0.05	1
$f_{\text{gas}}-T$	0.34 ± 0.22	
	0.66 ± 0.34	

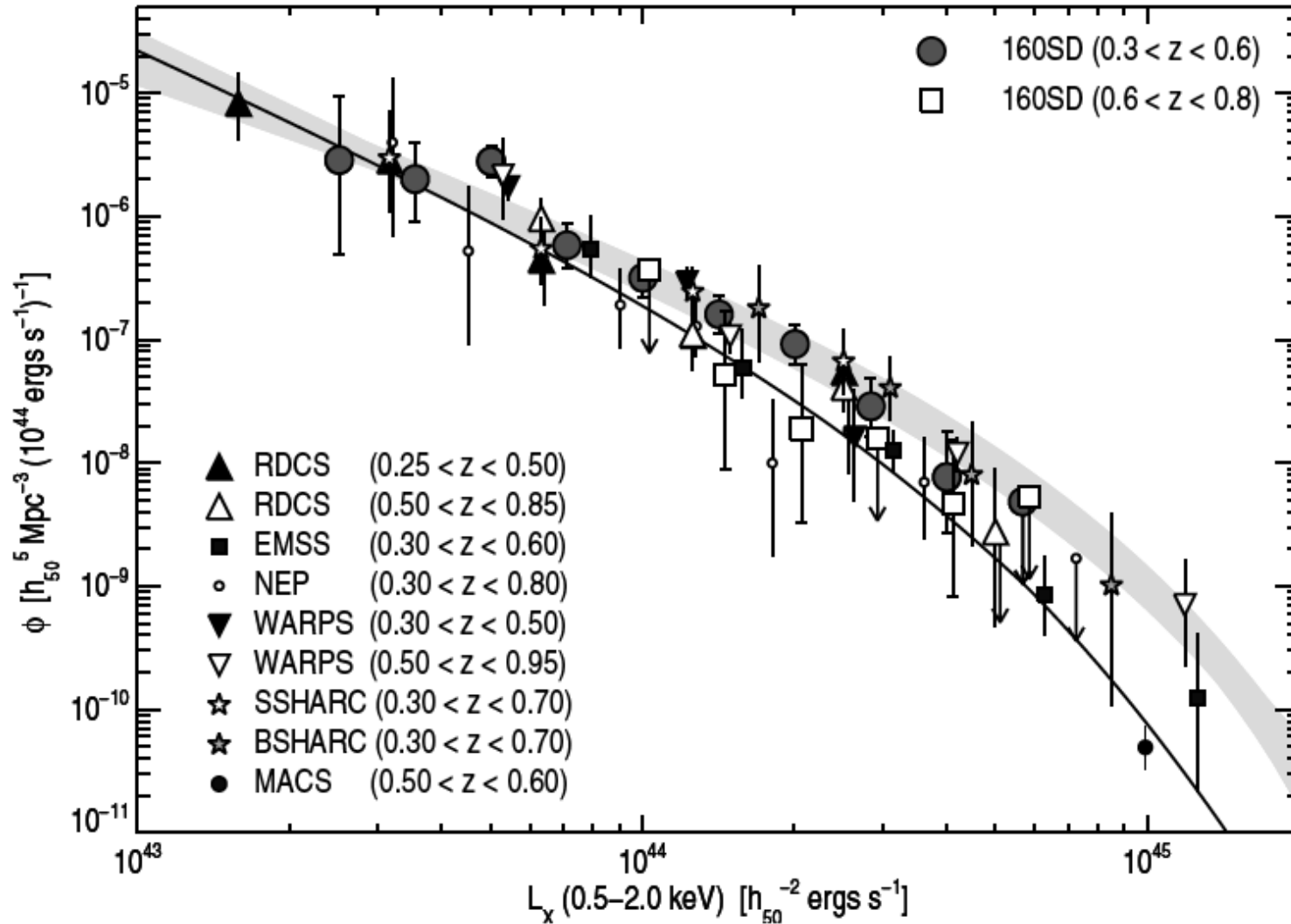
Observed X-Ray Scaling Relations for Clusters

Clusters as Cosmological Probes

- Given the number density of nearby clusters, we can calculate how many distant clusters we expect to see
- In a high density universe, clusters are just forming now, and we don't expect to find any distant ones
- In a low density universe, clusters began forming long ago, and we expect to find many distant ones
- Evolution of cluster abundances:
 - Structures grow more slowly in a low density universe, so we expect to see less evolution when we probe to large distances

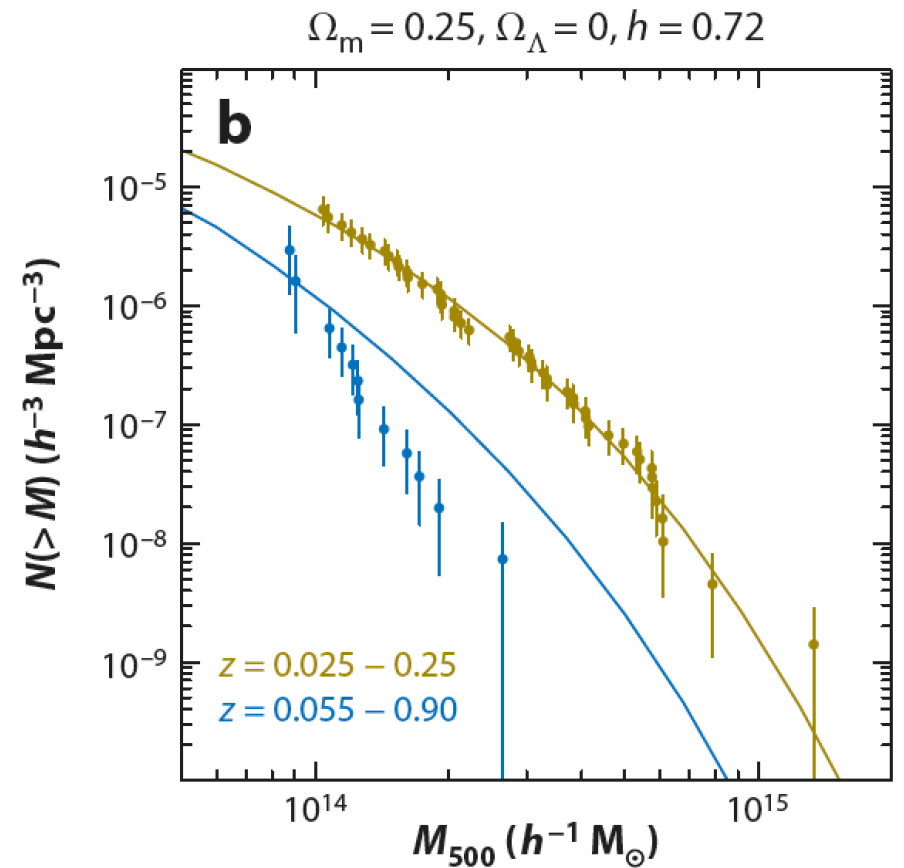
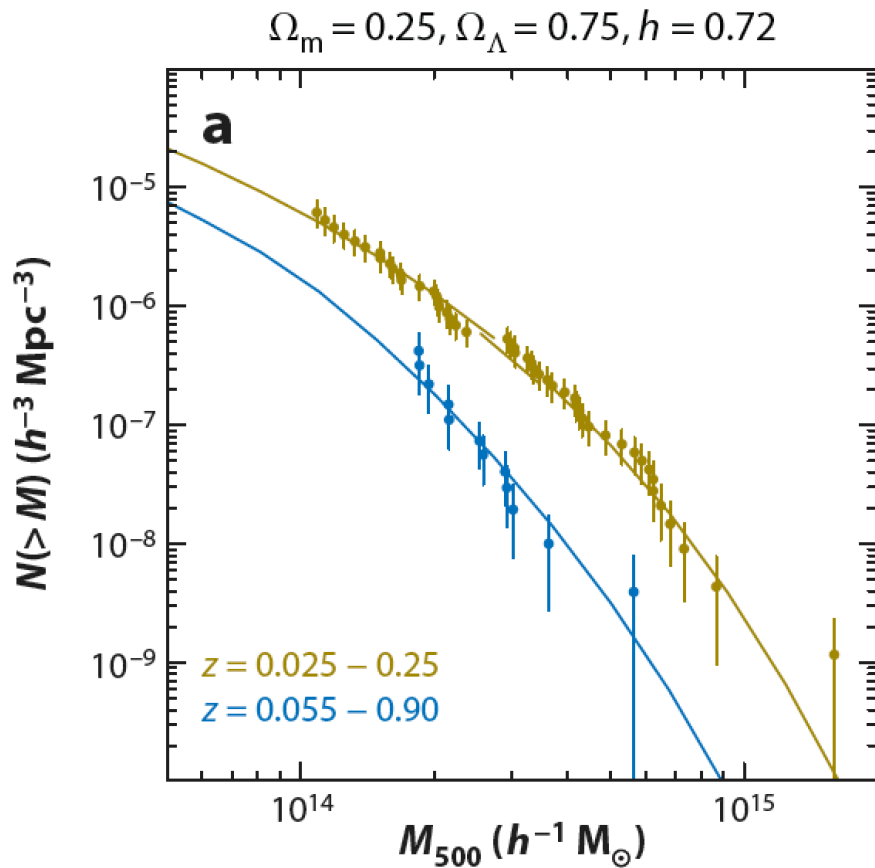


Evolution of the Cluster X-Ray Luminosity Function

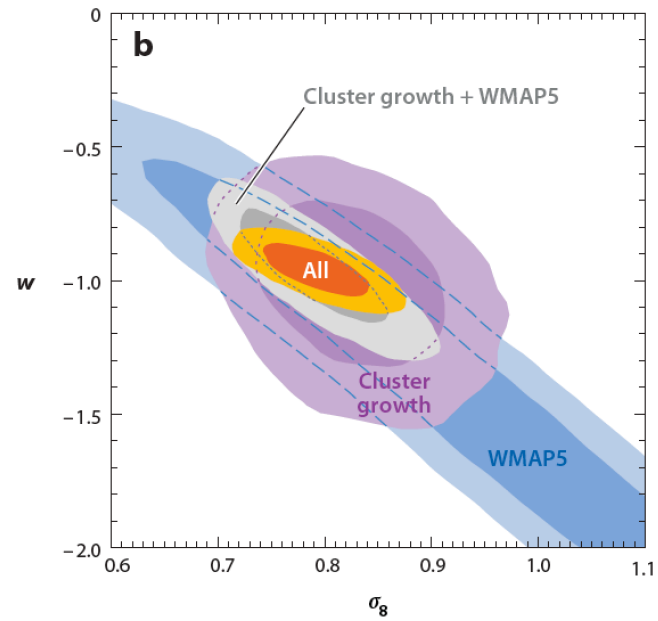
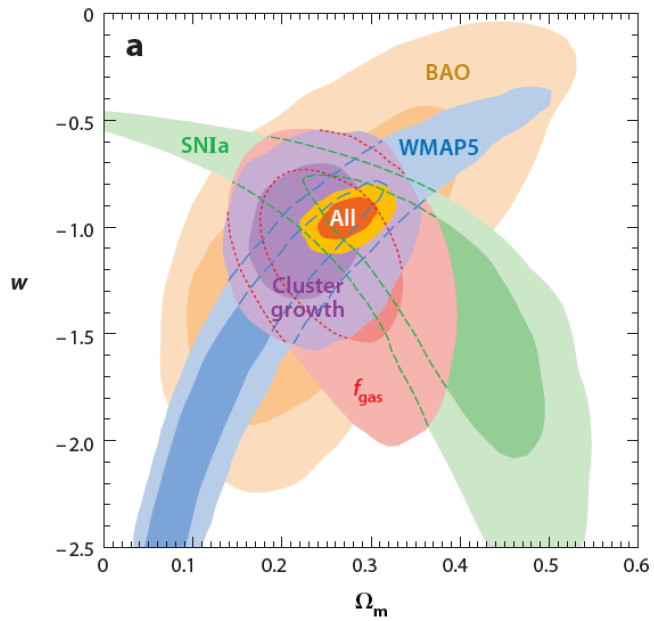
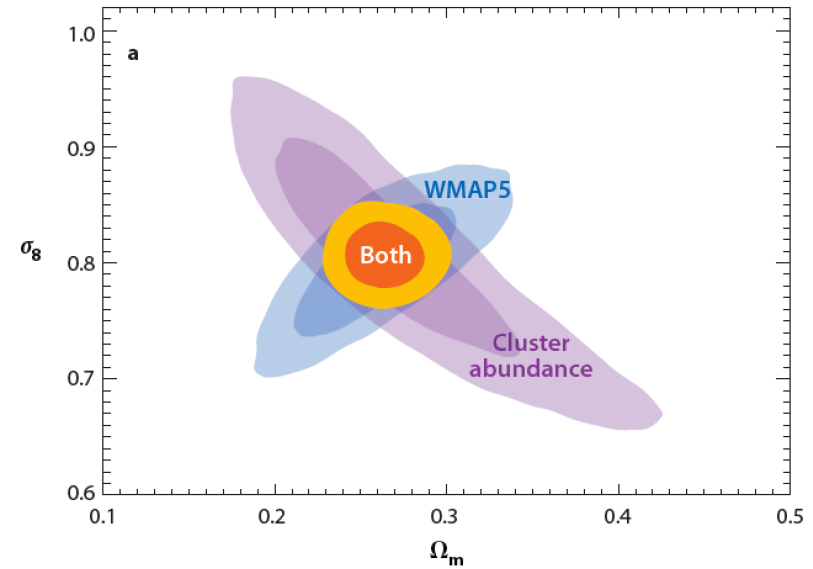
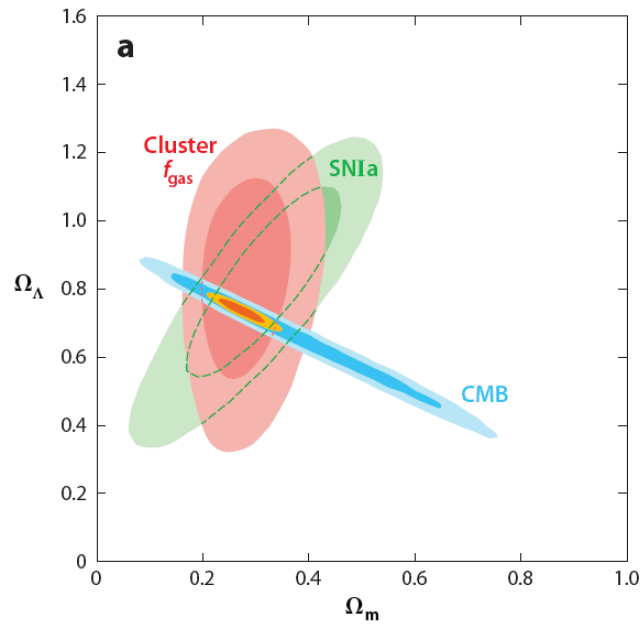


Clusters as Cosmological Probes

From the evolution of cluster abundance, expressed through their mass function:



Clusters as Cosmological Probes

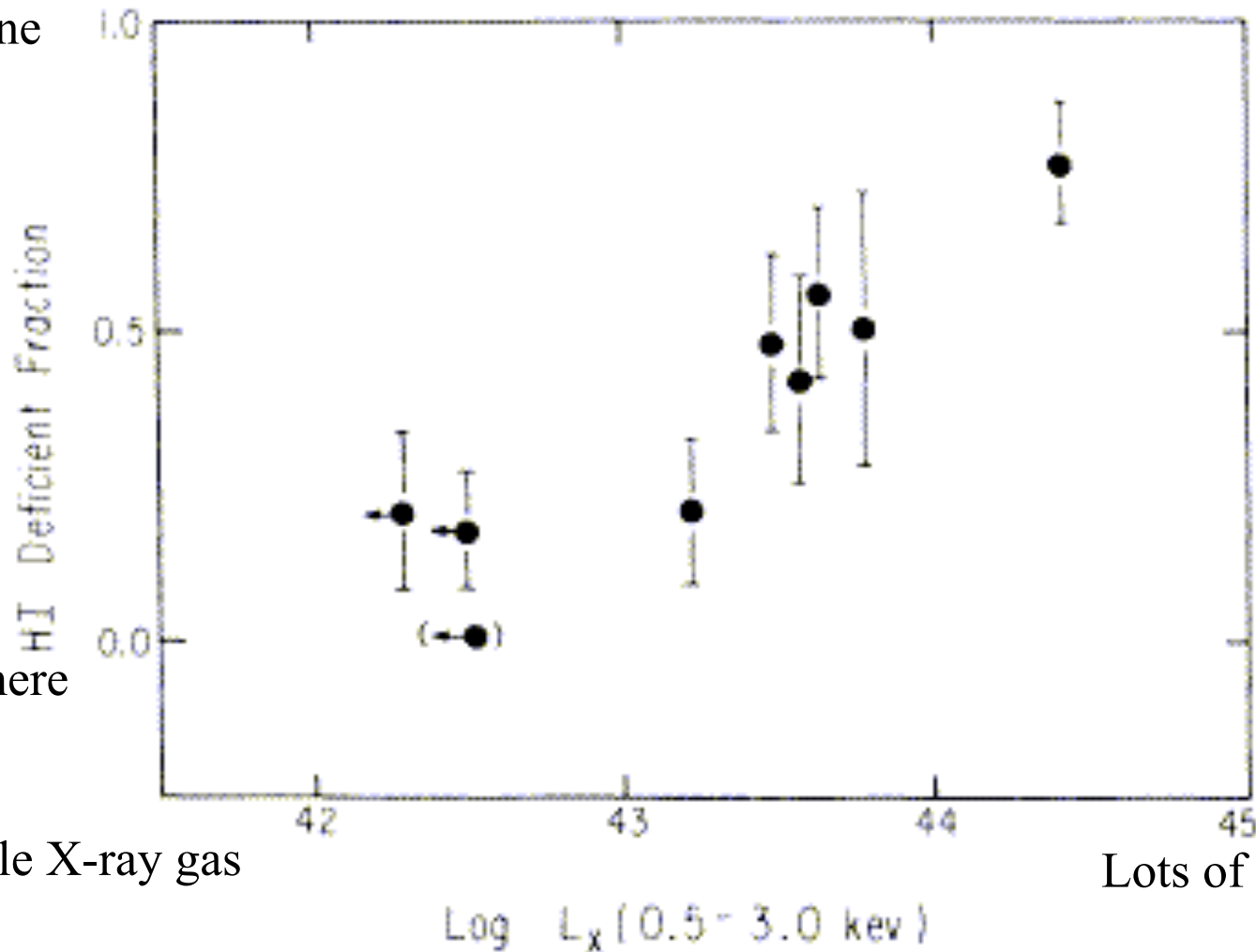


Hydrogen Gas Deficiency

- As gas-rich galaxies (i.e., spirals) fall into clusters, their cold ISM is ram-pressure stripped by the cluster X-ray gas
- Evidence for stripping of gas in cluster spirals has been found from HI measurements
- Most deficient spirals are found in cluster cores, where the X-ray gas is densest
- HI deficiency also correlates with X-ray luminosity (which correlates with cluster richness)
- It is the outer disks of the spirals that are missing
- Thus, evolution of disk galaxies can be greatly affected by their large-scale environment

HI Deficiency vs. X-ray Luminosity

All H I gone

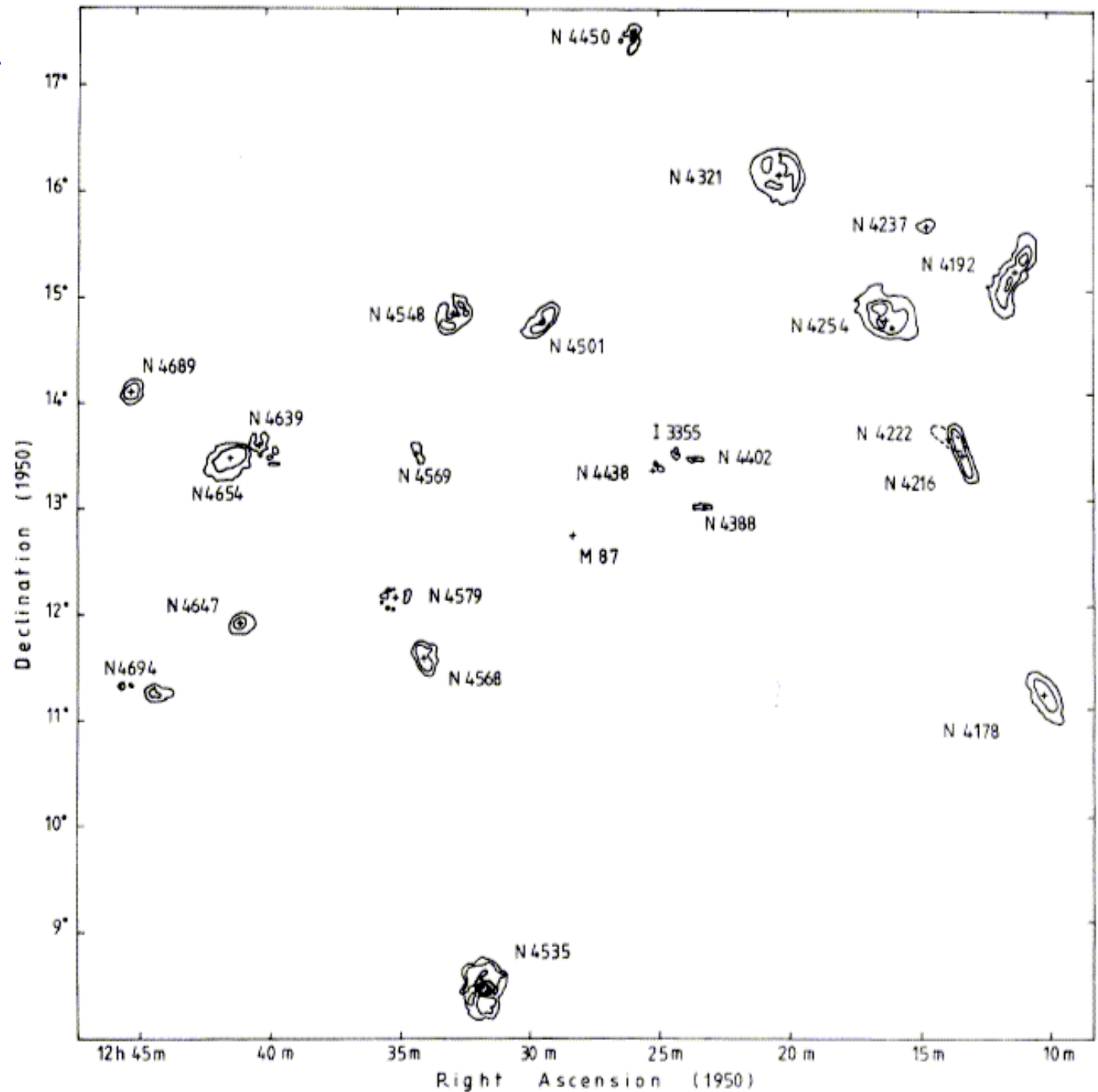


H I still there

FIG. 9.—Suggested relationship between the deficient fraction f , defined in the text, and the cluster X-ray luminosity in the 0.5–3.0 keV range.

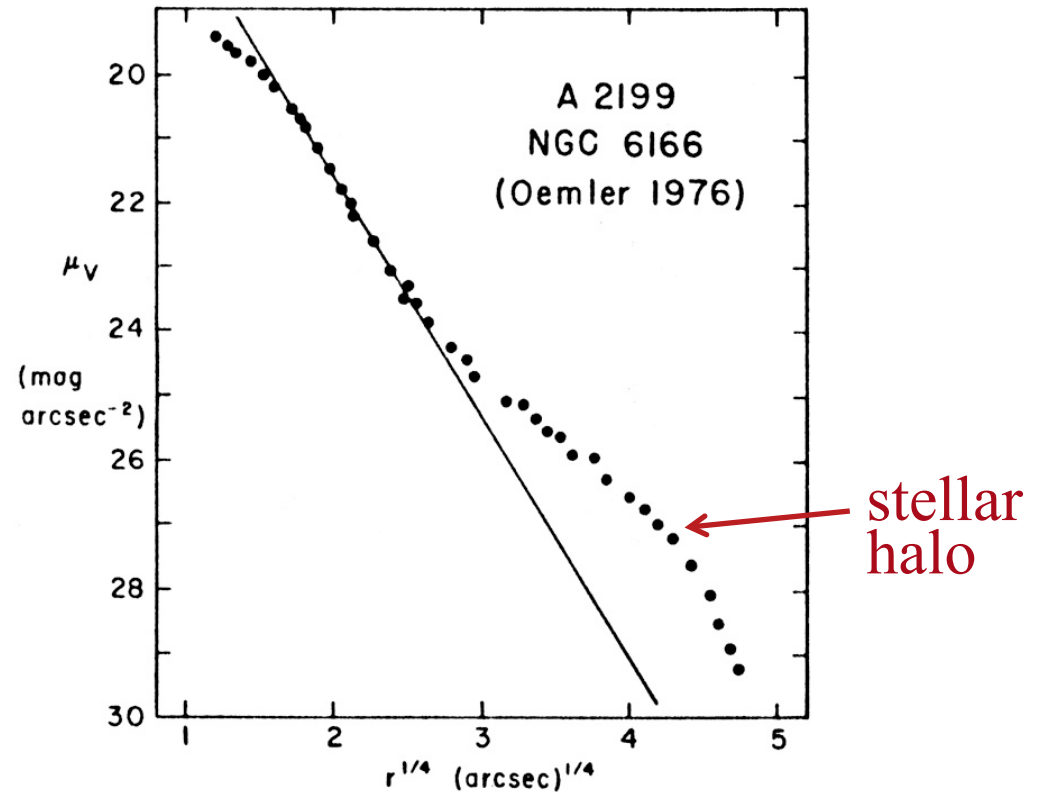
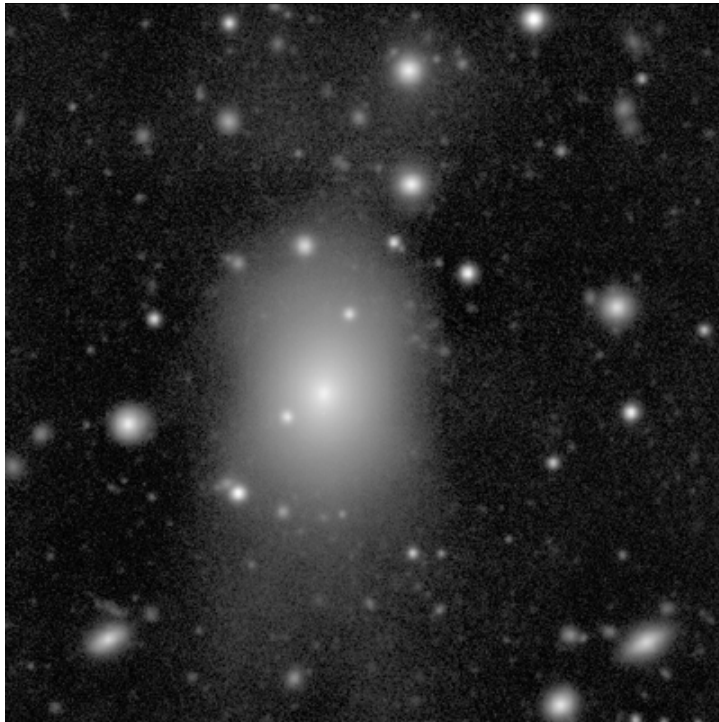
HI Map of the Virgo Cluster

Gaseous disks of spirals are much smaller closer to the cluster center



Central Dominant (cD) Galaxies in Clusters

Many clusters have a single, dominant central galaxy. These are always giant ellipticals (gE), but some have extra-large, diffuse envelopes - these are called cD galaxies

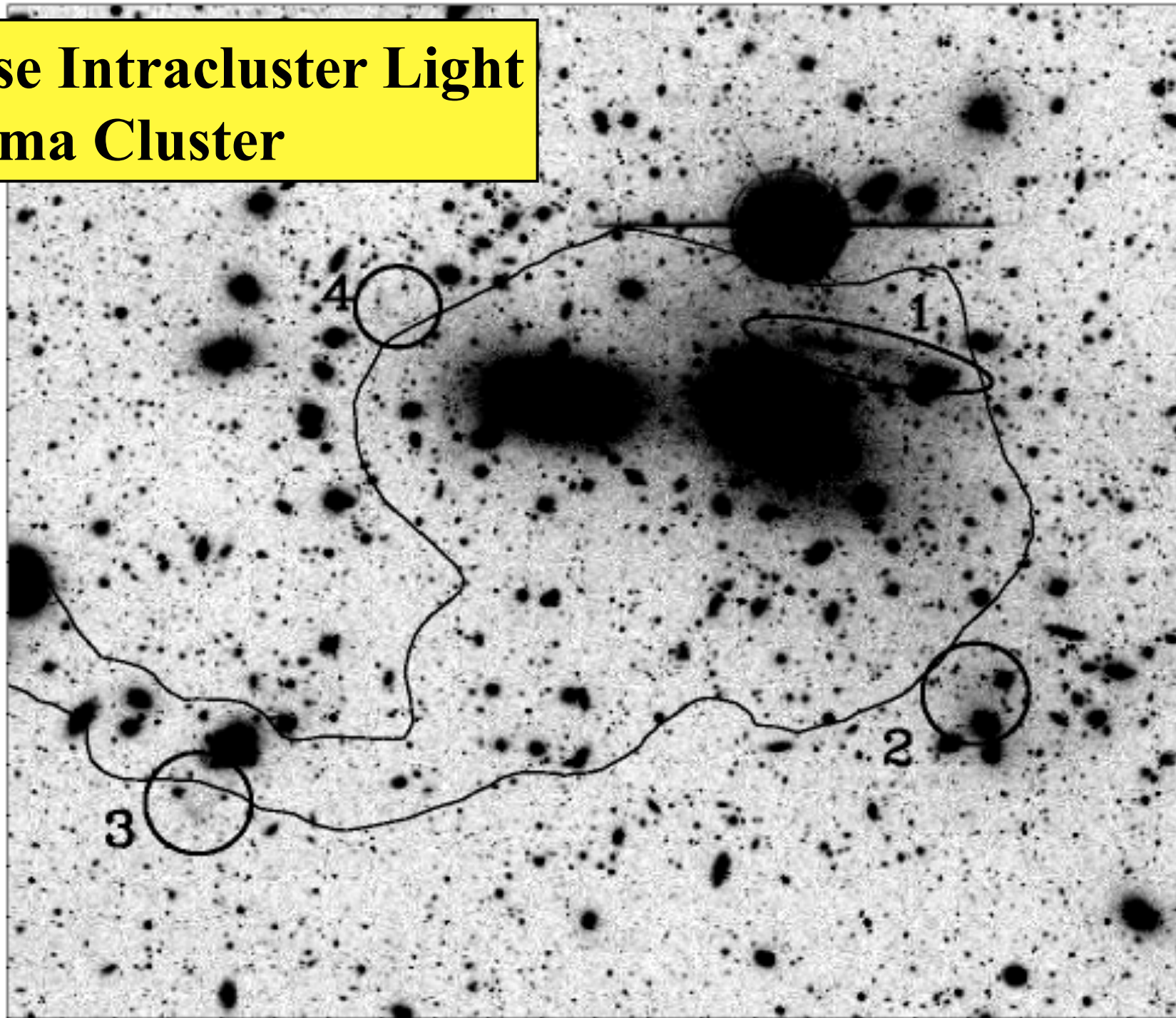


These envelopes are probably just “star piles”, a remainder of many tidal interactions of cluster galaxies, sharing the bottom of the potential well with the gE galaxy

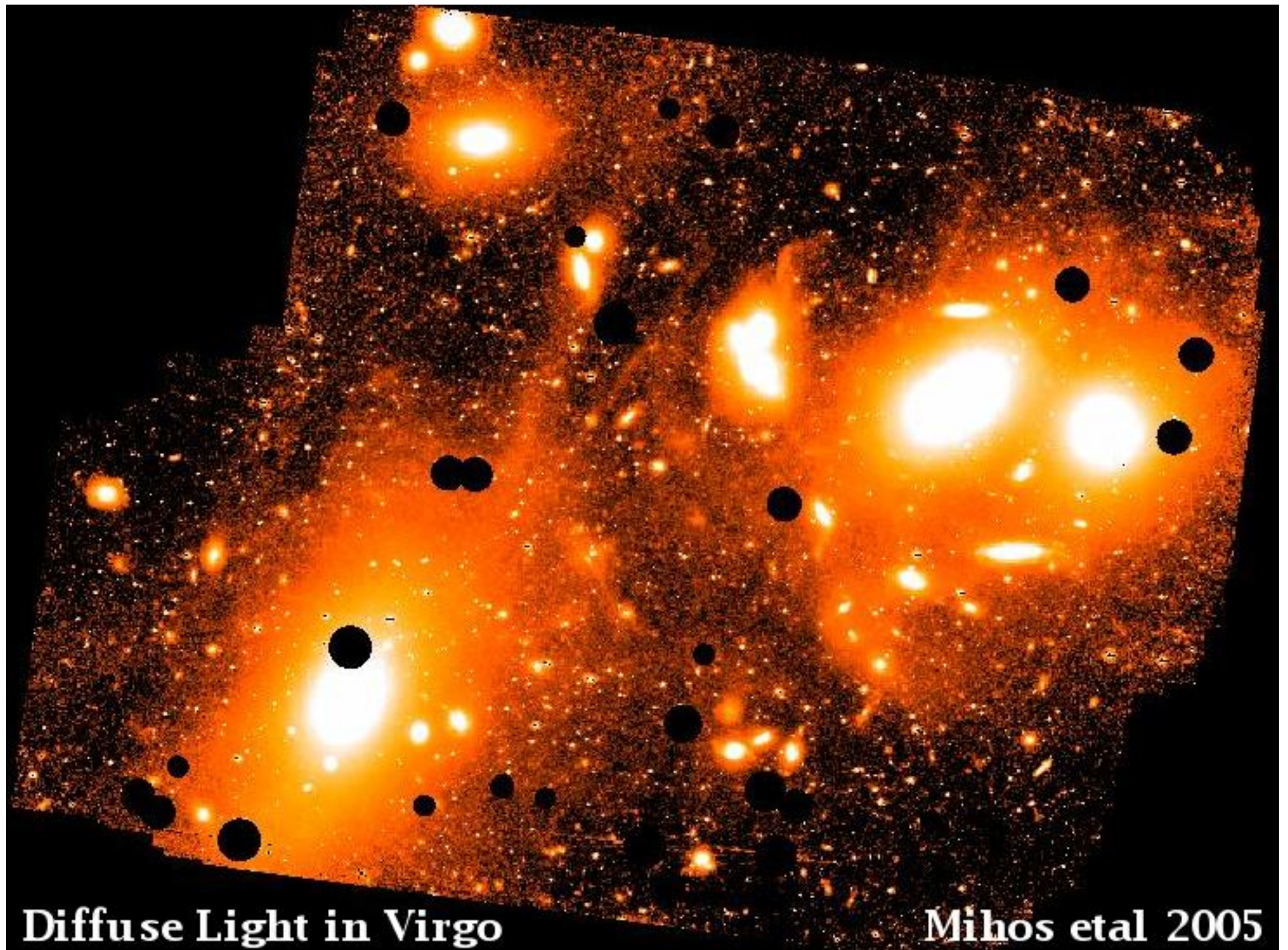
Intracluster Light

- Zwicky (yes, him again!) in 1951 first noted “an extended mass of luminous intergalactic matter of very low surface brightness” in Coma cluster
- Confirmed in 1998 by Gregg & West, features are extremely low surface brightness >27 mag per arcsec² in *R* band
- Also discoveries of intracluster red giant stars and intracluster planetary nebulae in Virgo & Fornax, up to ~ 10 -30% of the total cluster light
- Probably caused by galaxy-galaxy or galaxy-cluster potential tidal interactions, which do not result in outright mergers
 - This is called “galaxy harassment”
 - Another environment-dependent process affecting galaxy evolution

Diffuse Intracluster Light in Coma Cluster



*Gregg &
West
1998*



Diffuse Light in Virgo

Mihos et al 2005

Clusters of Galaxies: Summary

- Clusters are the largest bound (sometimes/partly virialized) elements of the LSS
 - A few Mpc across, contain $\sim 10^2 - 10^3$ galaxies, $M_{cl} \sim 10^{14} - 10^{15} M_{\odot}$
 - Contain dark matter ($\sim 80\%$), hot X-ray gas ($\sim 10\%$), galaxies ($\sim 10\%$)
 - This maps into discovery methods for clusters: galaxy overdensities, X-ray sources (via emission of SZ effect), weak lensing, etc.
- Clusters are still forming, via infall and merging
 - Studied using numerical simulations, with galaxies, gas, and DM
- Galaxy populations and evolution in clusters differ from the general field
 - While only $\sim 10 - 20\%$ of galaxies are in clusters today, $> 50\%$ of all galaxies are in clusters or groups
 - Clusters have higher fractions of E's and S0's relative to spirals
 - Interesting galaxy evolution processes happen in clusters

Supplementary Slides

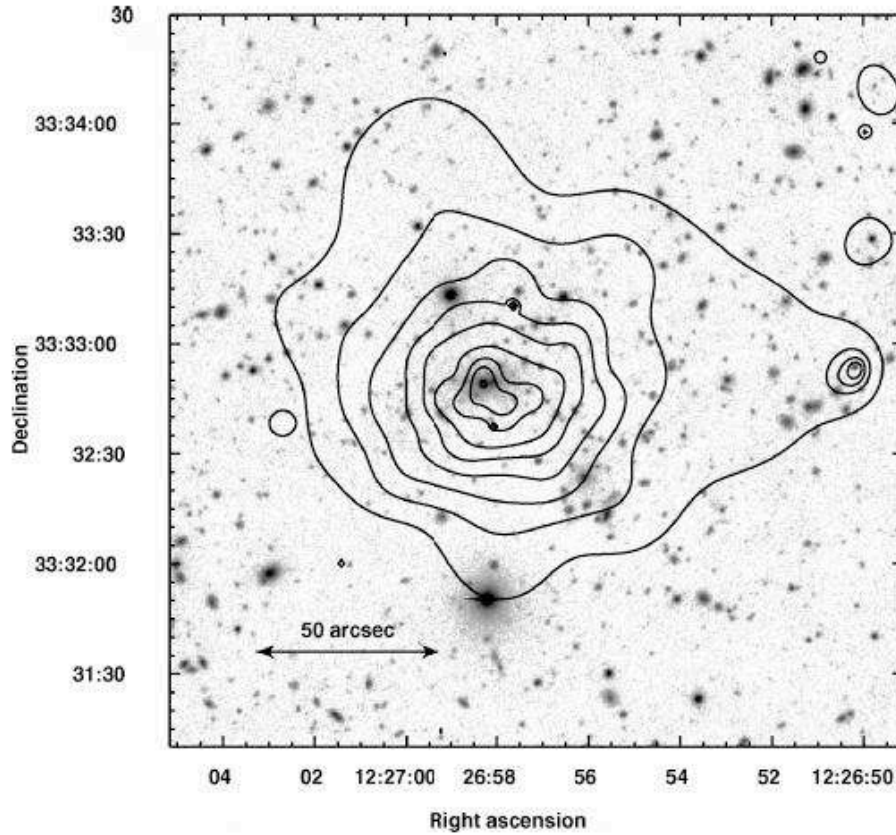


Fig. 6. – RXJ1226.9+3332, a relaxed massive cluster at $z = 0.89$. The contours of X-ray emission detected by *XMM-Newton* is overlaid on a Subaru I-band image. Figure from [37]

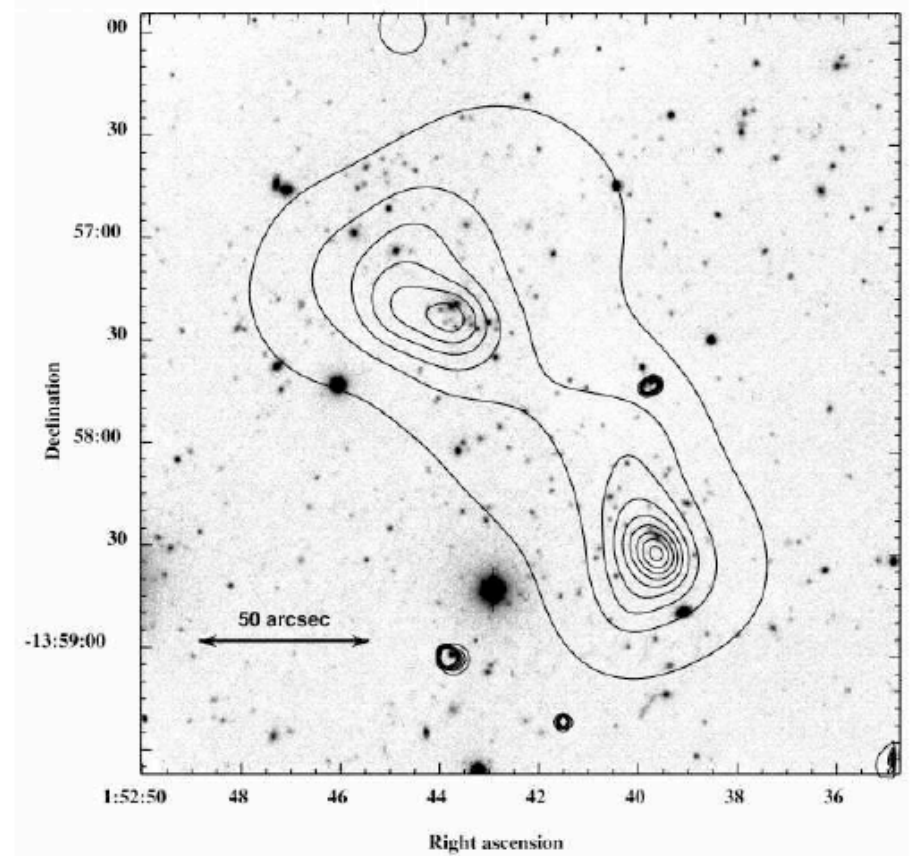
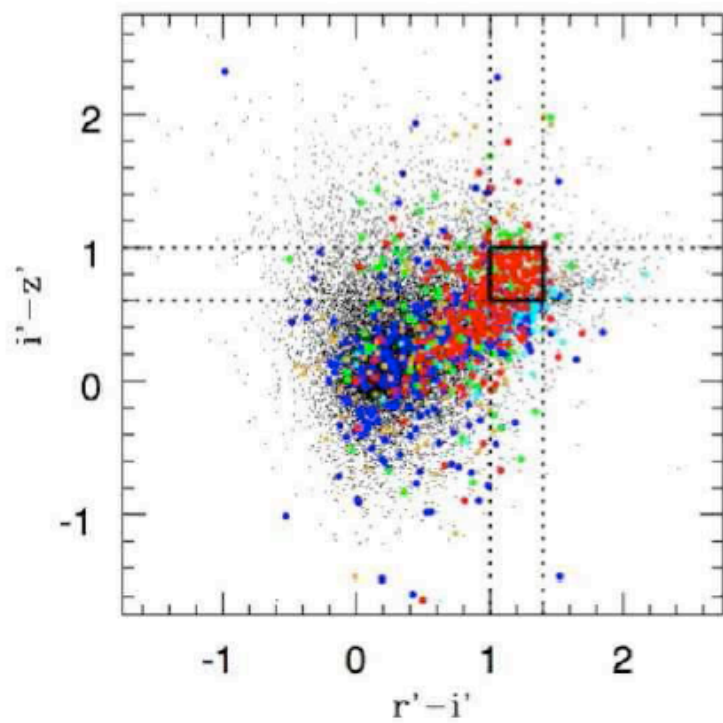
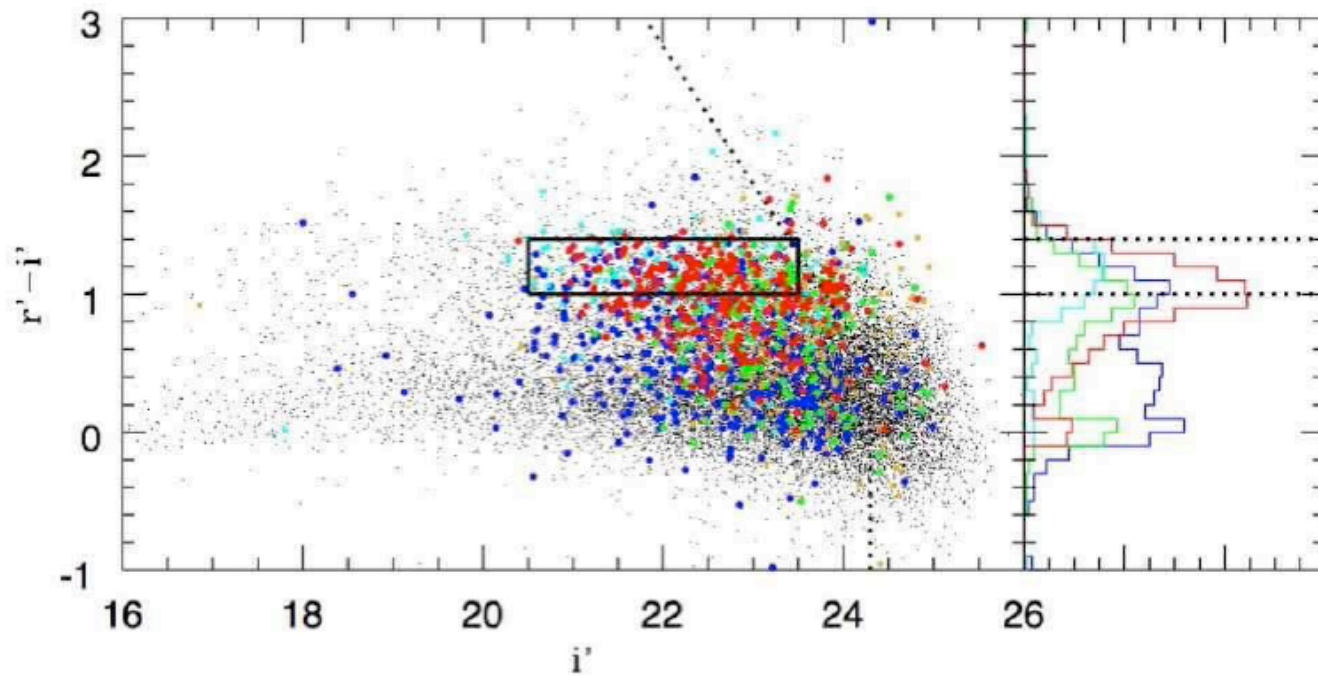


Fig. 7. – The merging cluster RX J0152.7-1357 at $z = 0.83$. The *Chandra* X-ray contours are overlaid on a Keck II I-band image. Figure from [26]. The *Chandra* temperature map shows a temperature increase between the two subclusters indicating that they have started to merge

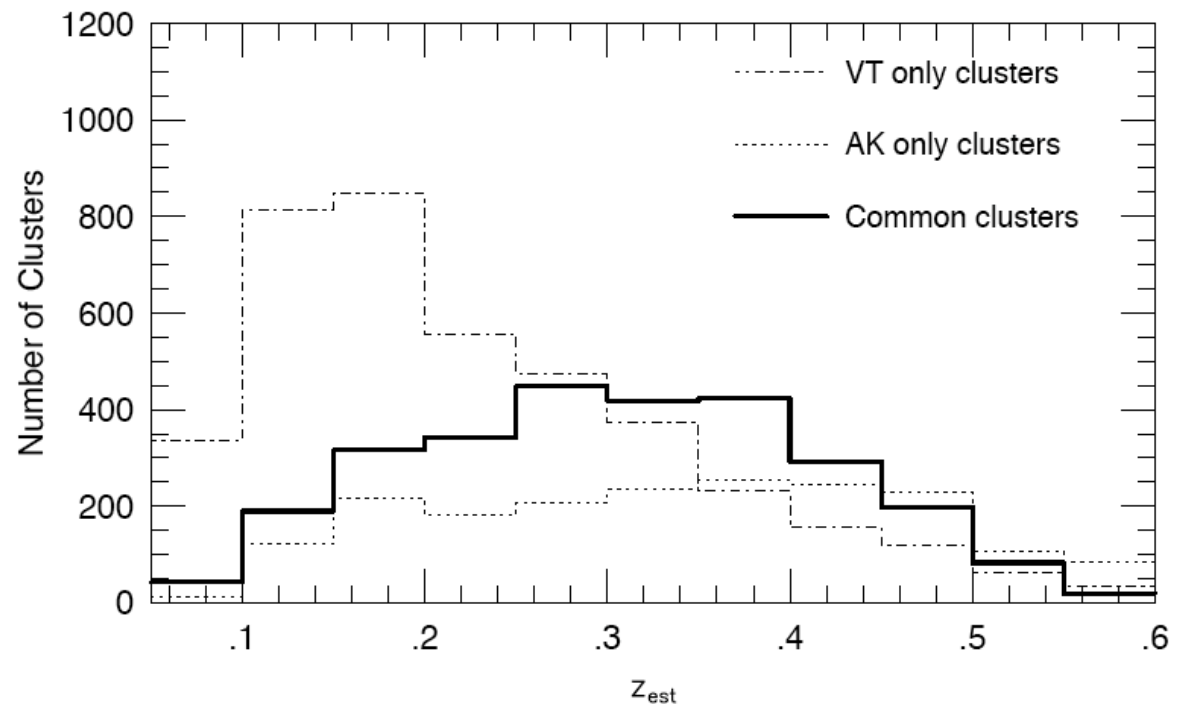
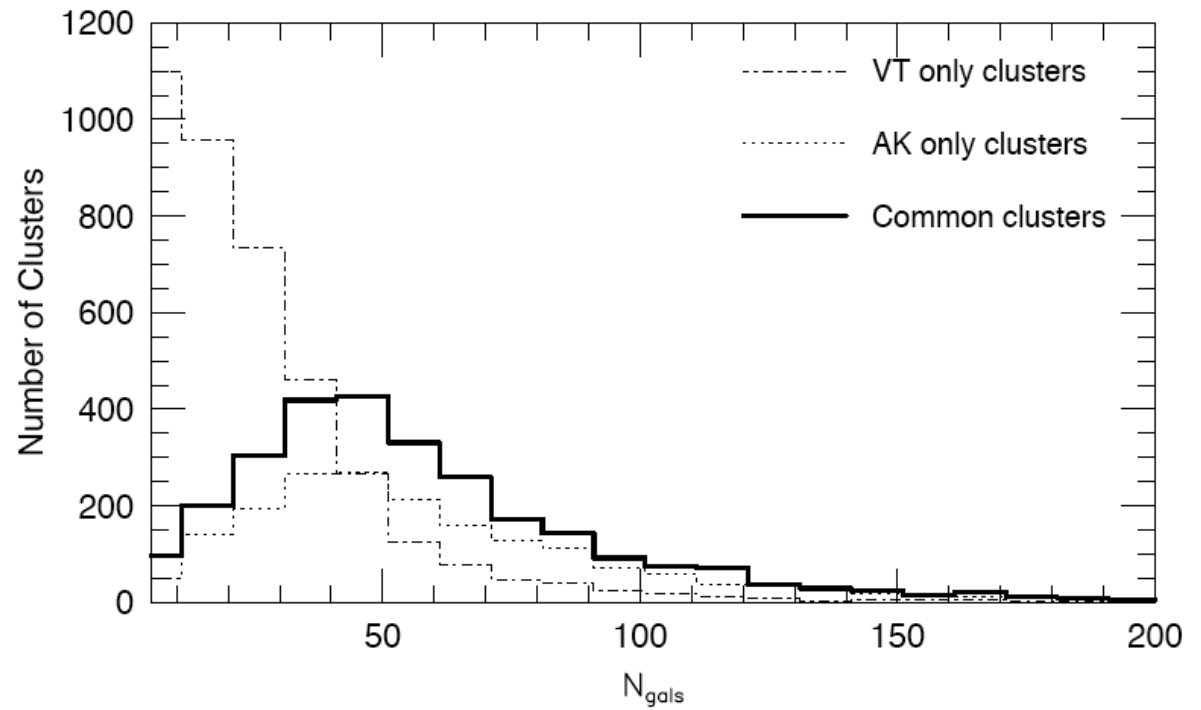


- Cluster Member
- $Z > Z_{\text{clus}}$
- $Z < Z_{\text{clus}}$
- Star
- No redshift

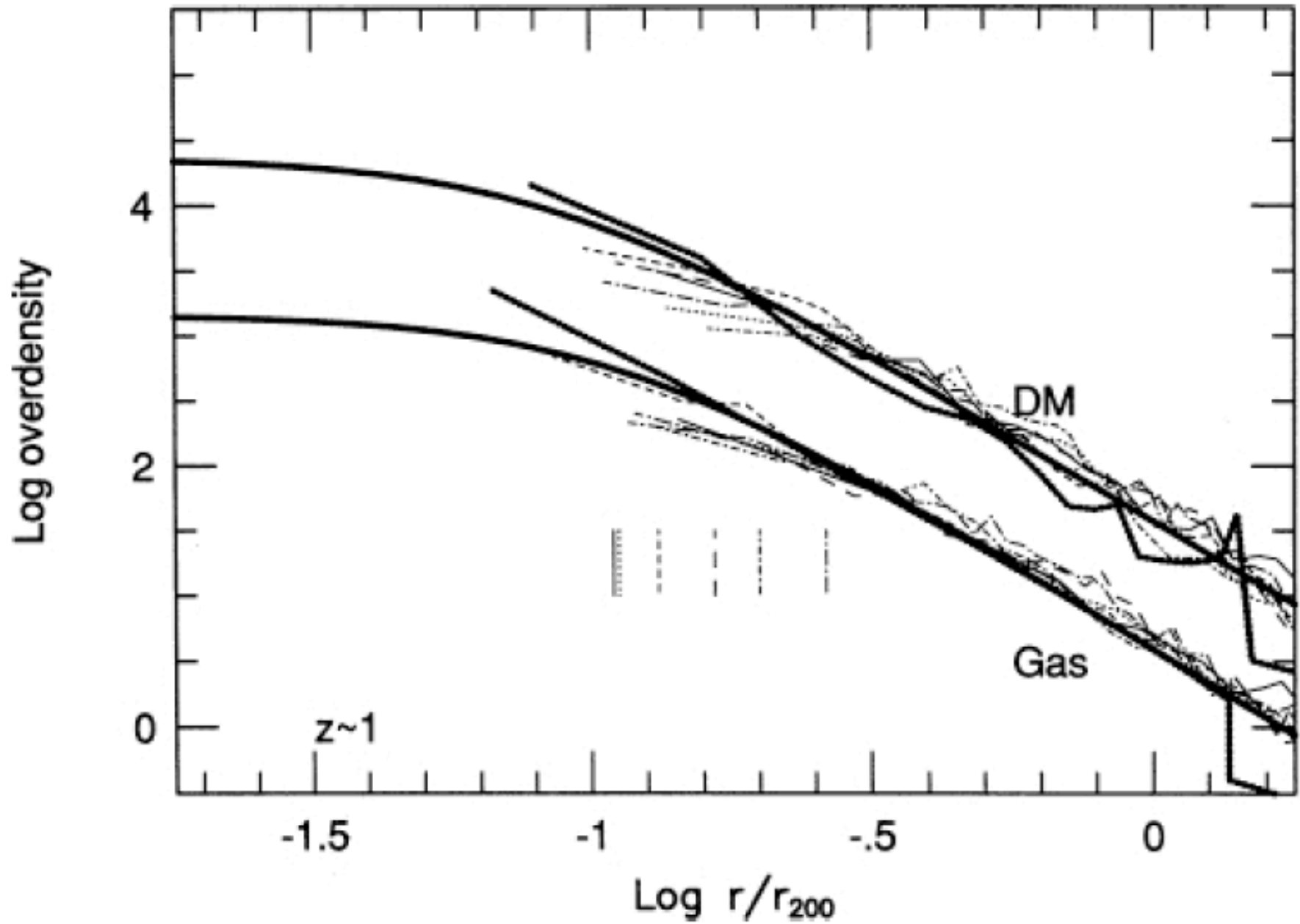
**Using Colors to Select
More Distant Clusters**

Comparing Different Selection Techniques

- Selection efficiency differs as a function of redshift, richness, etc.
- Optical and X-ray selections also differ: X-rays select dynamically older, more relaxed clusters



Predicted Cluster Density Profiles From Simulations



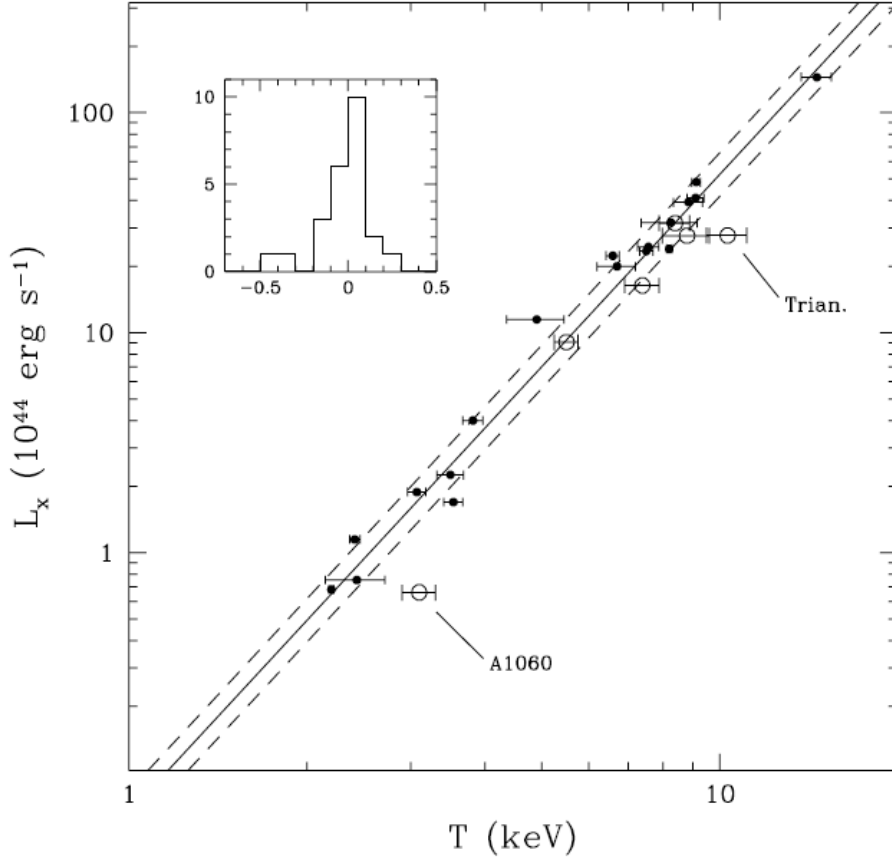


Fig. 16. – The relation between the bolometric luminosity and the temperature. Only clusters without strong cooling in the center are considered. The data are mostly from *GINGA* observations. The relation is steeper than expected in the standard self-similar model: $L_X \propto T^{2.88 \pm 0.15}$. Figure from [61].

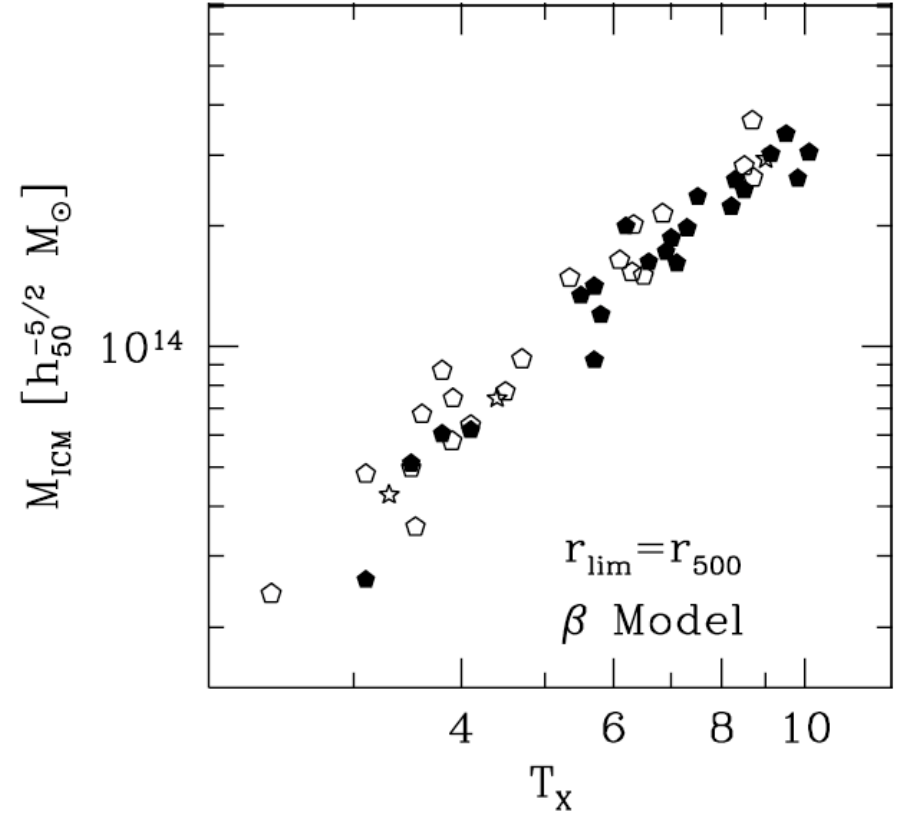


Fig. 17. – The relation between the gas mass and the temperature. The gas mass was measured with *ROSAT* and estimated within R_{500} . The temperature was measured with the *ASCA* or earlier missions. The relation is steeper than expected in the standard self-similar model: $M_{\text{gas}} \propto T^{1.98 \pm 0.18}$. Figure from [62].

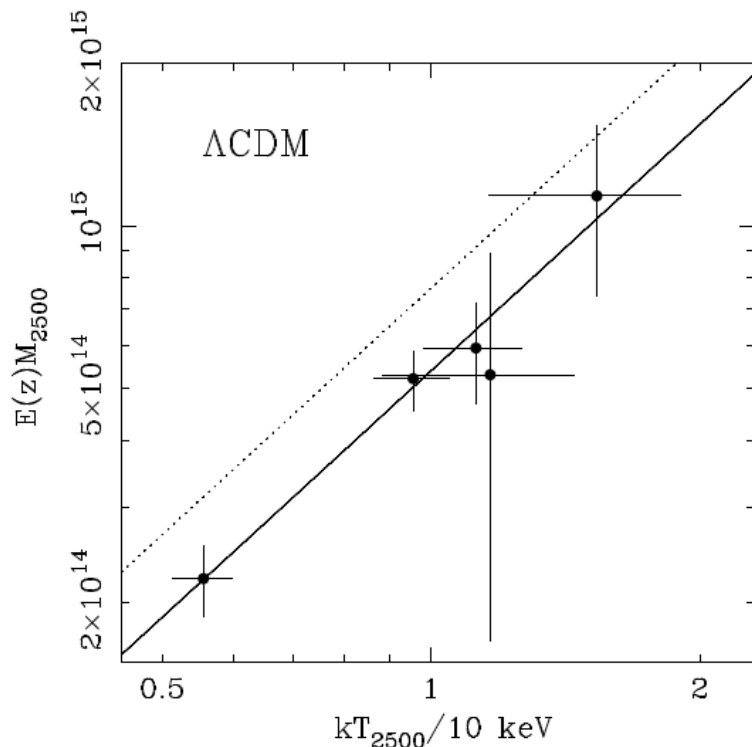


Fig. 21. – The $M_{2500}-T$ relation observed with *Chandra* for hot clusters. Solid line: The best fit power law, $M_{2500} \propto T_{2500}^{1.51 \pm 0.27}$. Dashed line: the predicted relation from adiabatic numerical simulations [68]. Figure from [81].

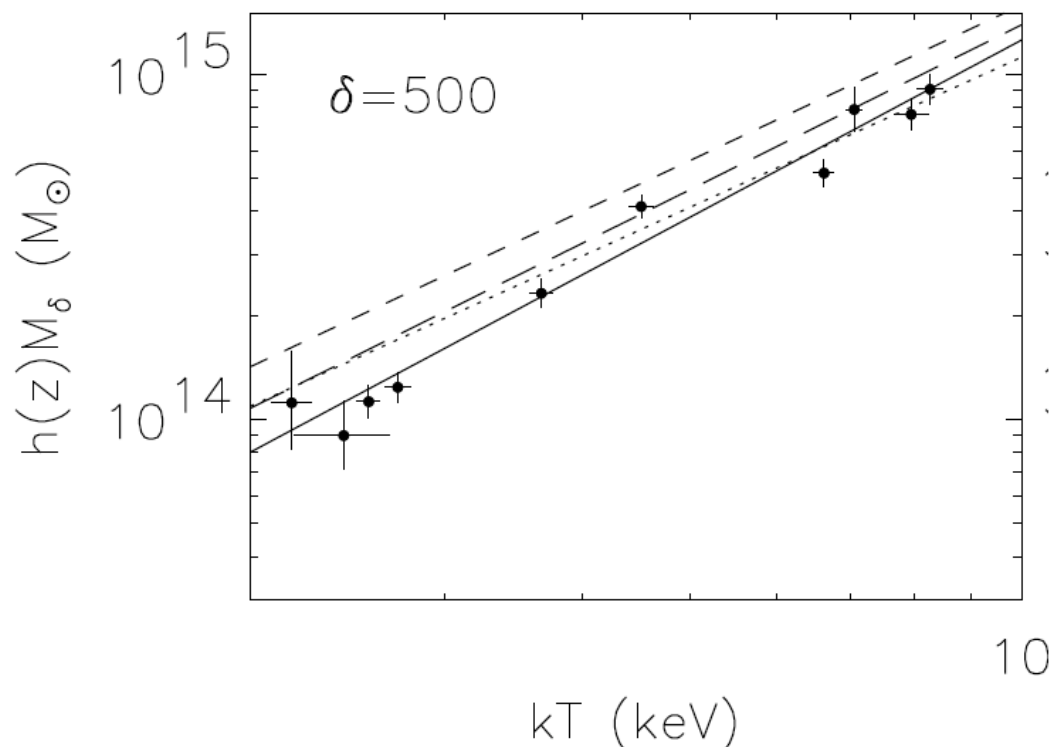
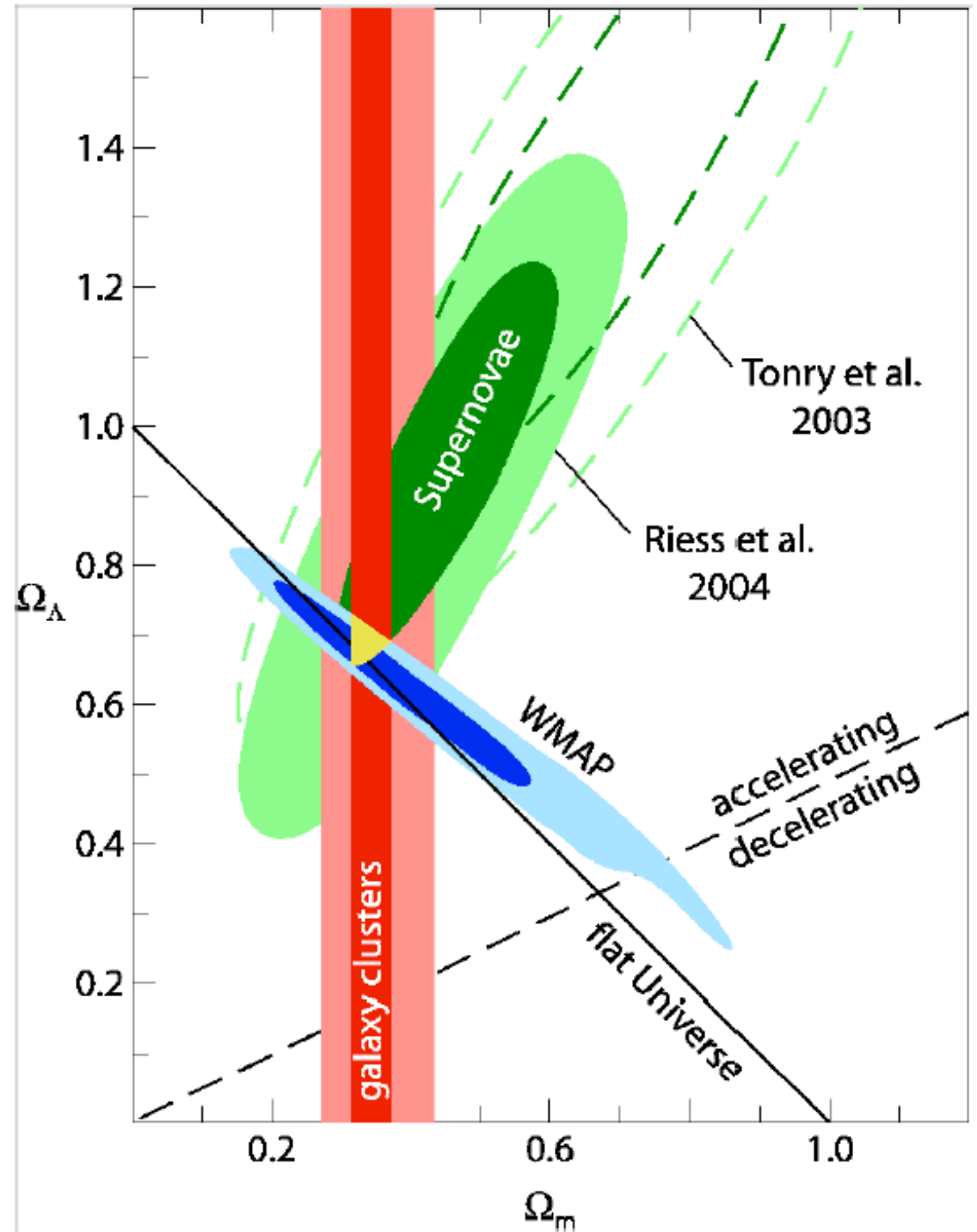


Fig. 22. – The $M_{500}-T$ relation observed with *XMM-Newton*. Solid line: The best fit power law for the whole sample. Dotted line: same for the hot cluster subsample. Dashed line: the predicted relation from adiabatic numerical simulations [68]. Long-dashed line: the relation derived from a numerical simulation including radiative cooling, star formation and SN feedback [125]. Figure from [124].

Evolution of the Cluster Abundance as a Cosmological Constraint



Ω_m From Baryonic Fraction and BBNS

27

X-RAY OBSERVATIONS OF CLUSTERS OF GALAXIES

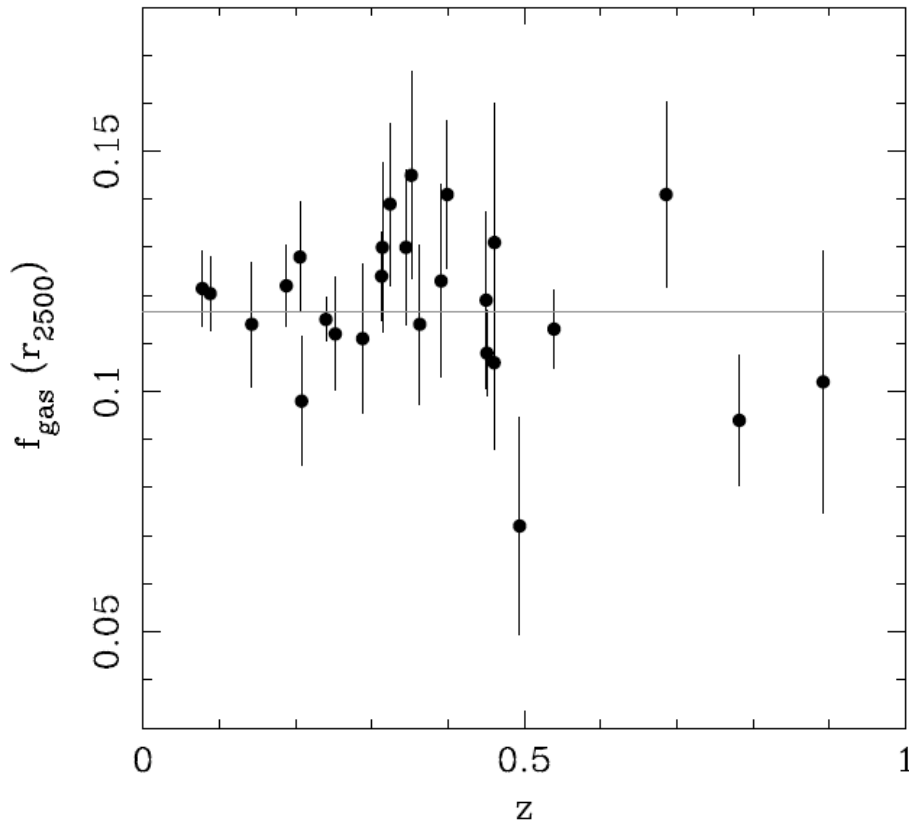


Fig. 25. – The X-ray gas mass fraction (1σ errors) versus z for a Λ CDM cosmology with $\Omega_m = 0.25, \Omega_\Lambda = 0.96$. In this 'best fit' cosmology f_{gas} is constant. Figure from [135].

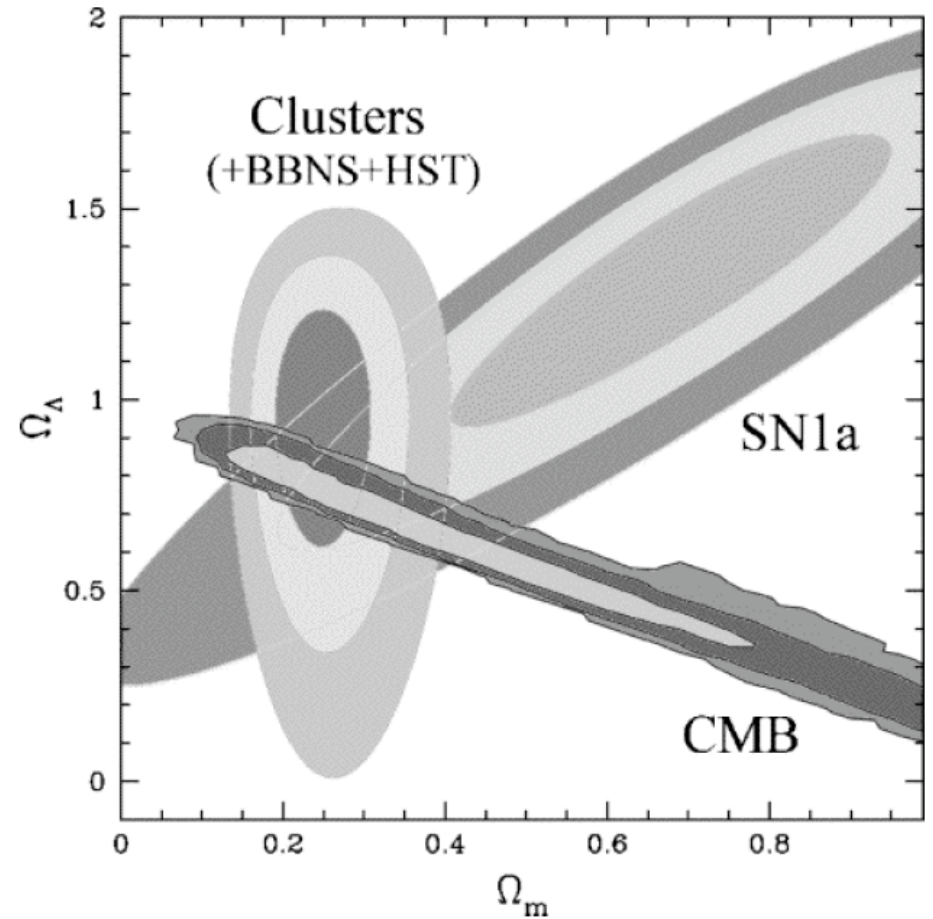
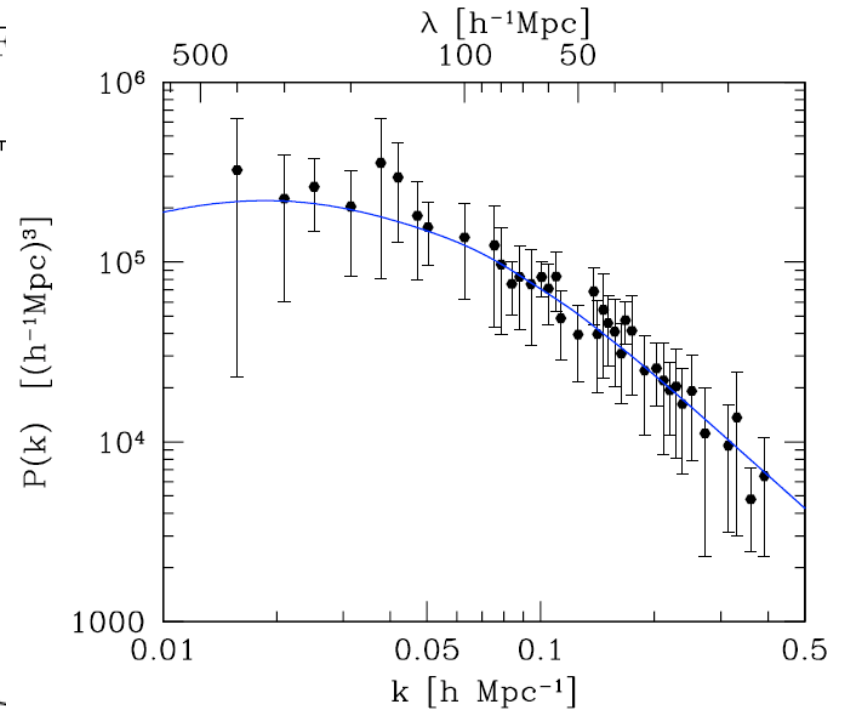
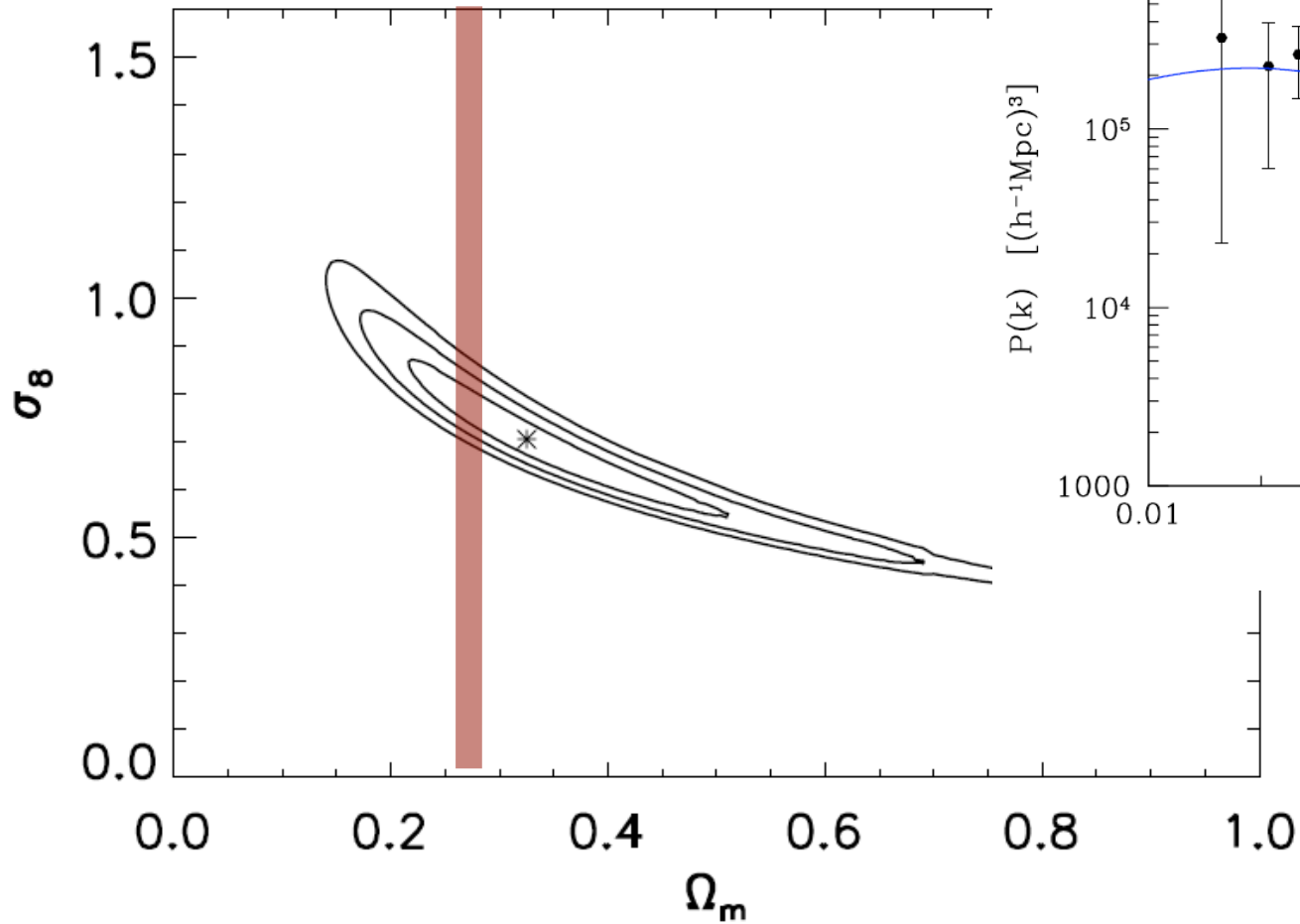


Fig. 26. – The $1, 2$ and 3σ confidence constraints in the Ω_m, Ω_Λ plane obtained from the analysis of the cluster f_{gas} data. Also shown are the independent results obtained from CMB and SNI data. Figure from [135]

X-RAY OBSERVATIONS OF CLUSTERS OF



Normalization of the LSS Power Spectrum

Fig. 32. – Likelihood contours (1–3 σ levels) in the σ_8 – Ω_m plane obtained from the REFLEX cluster abundances. Note the degeneracy between σ_8 and Ω_m . Figure from [174]

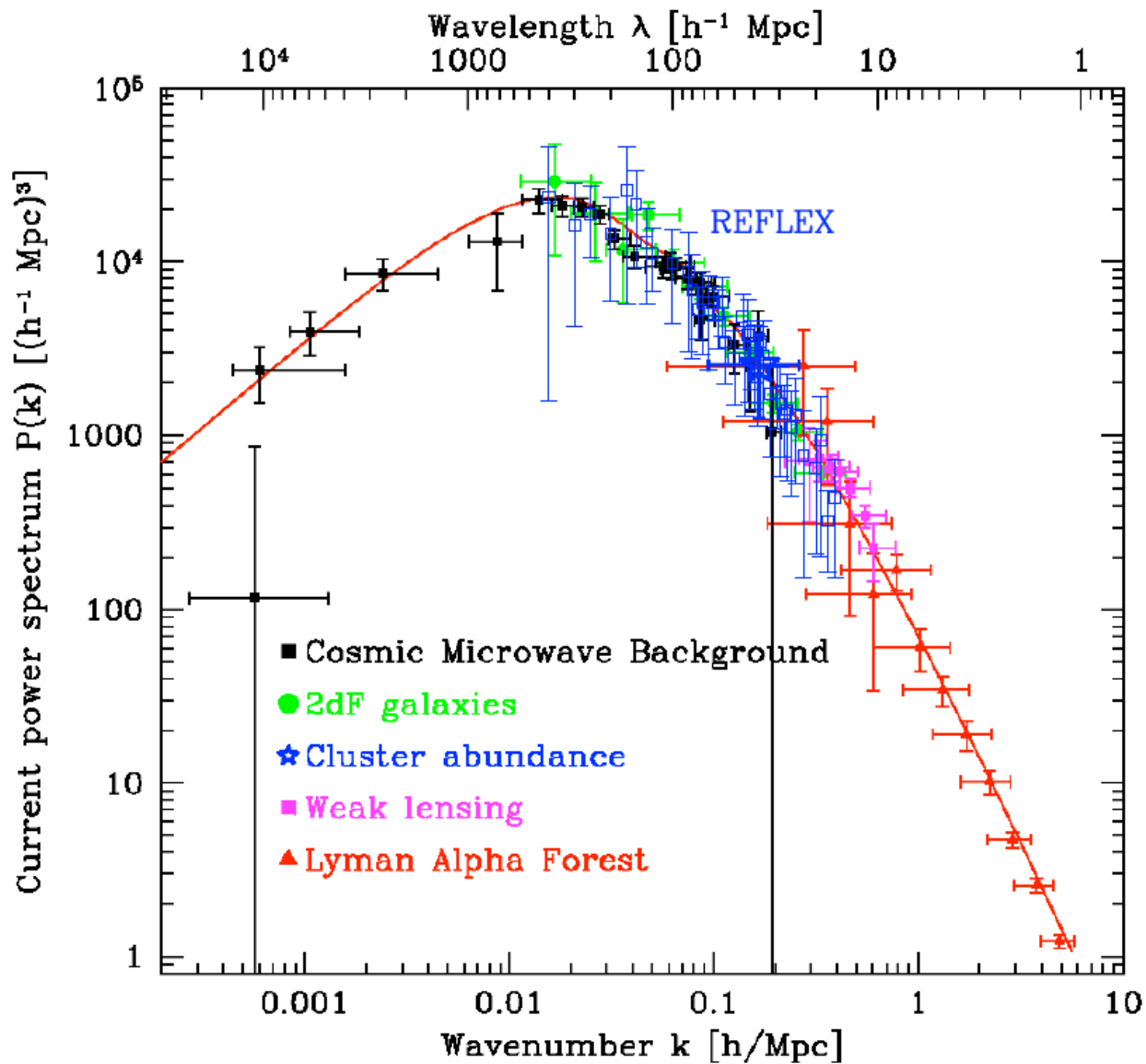


Figure 3: Compilation of fluctuation power spectra of various cosmological objects as compiled by Tegmark & Zaldarriaga (2002) with the added REFLEX power spectrum. The continuous line represents the concordance Λ CDM structure formation model.